

Improving urban thermal environments by analysing sensible heat flux patterns in zoning districts

You Jin Kwon ^{a,*}, Dong Kun Lee ^{b,*}, Jun-Hyun Kim ^c, Kyushik Oh ^d

^a Living Environment Research Center, Korea Institute of Civil engineering and building Technology, Korea, 1190, Simindae-Ro, Ilsanseo-Gu, Goyang-Si Gyeonggi-do, 411-712, 10223, Republic of Korea

^b Department of Landscape Architecture and Rural System Engineering, Seoul National University, Korea, 200 Gwanak-ro 1, room 9219, Gwanak-gu, Seoul 08826, Republic of Korea

^c School of Planning, Design & Construction, Michigan State University, 552 W Circle Dr., Rm 201H, East Lansing, MI 48824, United States of America

^d Department of Urban Planning and Engineering, Engineering Science & Technical Building, Hanyang University, 222 Wangsimni-ro, Seongdong-gu 04763, Republic of Korea

ARTICLE INFO

Keywords:

Sensible heat flux
Land cover
Thermal zoning
Thermal environmental analysis
Energy budget

ABSTRACT

This study developed a method of improving Seoul's thermal environment by focusing on sensible heat flux and types of land-use and cover to mitigate the urban heat island (UHI) effect. First, the relationships between the sensible heat flux in summer and (a) the land cover ratio, and (b) the heights and densities of buildings in different land-use zoning districts were identified and analysed. The rationale for improving the thermal environment was then considered based on the physical relationships among heat, space, and the thermal-environment type. Energy budget distribution data were then used to identify an optimised land-use plan to mitigate the UHI effect. Spatial data describing the physical elements in land-use zoning were then generated using high-resolution images of the sensible heat flux distribution and directly correlated to existing land-use and thermal comfort. Finally, a K-means clustering analysis was employed to determine the unfavourable and favourable thermal areas in each zoning district based on correlated sensible heat flux data. The results indicate that the highest concentration of unfavourable thermal areas of all studied zoning districts was neighbourhood commercial districts, which accounted for 9.9% of the total identified unfavourable thermal areas, whereas the lowest level of sensible heat flux was observed in single-family residential areas. This study thus developed a basis for a spatial planning framework that can be used to improve the thermal conditions of cities and encourage summer energy savings using zoning-based requirements.

1. Introduction

More than 60% of the global population is expected to reside in urban areas by the end of the century (Jiang & O'Neill, 2017). This increasing urbanisation should also be examined in terms of the changing social expectations associated with land-use (Roweis & Scott, 1981). The consequences of urbanisation and urban degradation resulting from urban development have been well documented throughout the capitalist social integration process (Dear & Scott, 1981). In addition to the trend of rapid urbanisation, urban implosion is increasing the density of the urban population, particularly in warmer climates (Coutts et al., 2007). These ongoing changes ensure that the urban heat island (UHI) effect is persistent in global cities (Grimm et al., 2015), worsening the quality of urban environments. Through

unintended changes to the local climate, the UHI effect requires residents to maintain comfort levels using heating, ventilation, and air conditioning (HVAC) systems, thus consuming more energy and generating even more heat. To address issues such as the UHI effect and its associated increased energy usage, sustainable urban development has been promoted as an ultimate goal of urban planning and/or environmental policy, such that the efforts of many modern cities toward healthy and smart city goals are based on the concept of sustainability (Y.J. Kwon et al., 2019; Ramaswami et al., 2016). Research has shown that, by using natural urban amenities such as mountains and rivers, it is possible to achieve energy sustainability while preserving the urban environment (Baum et al., 2007).

It is important to note that environmental deterioration is not only detrimental to the quality of the urban natural and built environments,

* Corresponding authors.

E-mail addresses: eugene.kwon@kict.re.kr (Y.J. Kwon), dklee7@snu.ac.kr (D.K. Lee).

but also to the health of residents (Zhao & Li, 2017), particularly the elderly, who are especially vulnerable to extreme temperatures. As the populations of many nations begin to age, it is necessary to develop urban environmental policies that protect the increasing numbers of elderly residents (Buffel & Phillipson, 2016). Additionally, thermal environmental issues are increasing in importance as the size of the UHI effect expands with continued urbanisation (Tran et al., 2006). Given that zoning systems impact the spatial organisation of cities, it is necessary to review zoning procedures and requirements to determine how they may be used to mitigate urban heat generation in the summer (Baker et al., 2002), as this trend has a detrimental effect on the thermal comfort of urban residents.

The negative effects of urban heat generation are consequences of heat exchange causing temperature changes. Understanding the relationship between heat flux and land cover is critical for identifying methods of reducing heat generation in urban areas (Y.J. Kwon et al., 2019). The sensible heat flux (Q_h) is a major factor that influences the urban energy budget, which is the exchange of heat between the surface and the atmosphere (Stull, 2015), and provides an efficient way to differentiate the physical attributes of various surfaces (Y.J. Kwon et al., 2020) and quantitatively assess the heat transfer that affects temperature (J.A. Voogt & Grimmond, 2010; Zhuang et al., 2016). In this study, we accordingly defined thermal zoning as the distinction of favourable thermal areas that should be preserved from unfavourable thermal areas that require advancement. Previous research on spatial typification based on the energy budget has defined favourable thermal areas (FTAs) as areas with low Q_h , whereas unfavourable thermal areas (UTAs) are spatially concentrated areas with elevated Q_h values (Y.J. Kwon et al., 2019). Therefore, we investigated an approach to improving the urban thermal environment by addressing the interaction between the physical heat concept of Q_h and the surface compositions of different zoning districts.

1.1. Zoning and the thermal environment

Zoning is an important method of urban planning that, on a municipal level, facilitates the efficient management of land-use and urban activities (Fischel, 1999). In this way, zoning regulates the built-up environment to protect the welfare, health, and safety of the community (Mixon & Dougherty, 1999), and thus can be reasonably expanded to include environmental regulations (Lai, 1994). Urban zoning also affects urban economic activities including housing, the real estate market, social welfare, and local commercial businesses (Pogodzinski & Sass, 2017). As a result, the potential and assigned uses of urban land must be reviewed (Németh & Langhorst, 2014) in consideration of the detrimental effects of excessive land-use regulations (McLaughlin, 2012) and zoning, which can often conflict with the public interest. Given that sustainability should be the ultimate goal of efforts to improve overall urban welfare, a holistic view of land-use regulations and zoning should consider environmental issues in addition to economic and social issues (Gowdy, 2005; Norton, 2007). When determining the sustainability of a city, one must consider that ecosystem services, the direct and indirect contributions of the environment to human well-being, must be balanced with changes in land-use (Wu et al., 2013). However, current zoning methods overlook the effect of the thermal environment (Jusuf et al., 2007).

Despite limited urban land availability, most cities distinguish between areas for public and private use (Otubu, 1992). Recent studies of land-use in Smart City planning and regional planning efforts have only emphasised land-use efficiency (Grossi & Pianezzi, 2017; Neirotti et al., 2014) without any consideration for land surface cover, and even long-term urban planning typically focuses solely on sustainable land management (Zitti et al., 2015). Clearly, planners and policymakers tend to disregard the thermal environment created by surface composition in long-term spatial planning, including when defining zoning requirements.

Commercial and high-density residential zones are dominated by high-rise buildings that provide efficient land-use (Chan & Lee, 2009). The UHI effect is exacerbated in such districts because of the higher densities in terms of people, energy usage, and material types (Stewart & Oke, 2012). Nevertheless, most modern cities do not address the thermal conditions and instead continue to operate within zoning regulations that favour the housing market (Halleux et al., 2012; I. Kim et al., 2013; Gyourko et al., 2008). However, when considering the thermal effects on the welfare of residents, it is essential to identify the thermal distribution in sub-divisional districts and classify heat-related spaces that can be used to mitigate heat generation (Y.J. Kwon et al., 2018). Therefore, the objective of this study is to identify spatial patterns of Q_h based on urban land cover characteristics according to zoning district.

1.2. Research trends addressing urban heat, the thermal environment, and land cover in zoning

Other previous studies have focused on the relationships between heat, land cover, and use classification. Research pertaining to the thermal environment has been conducted at regional and urban scales using thermal maps of urban climate-sensitive zones for informed urban planning (Acero et al., 2013) and on the development of urban spatial typification based on the energy budget (Y.J. Kwon et al., 2018). Note that land cover type is also correlated with urban heat intensity. The results of previous studies on the relationships among urban land cover, heat, and building area vary. Most of these studies attempted to develop an urban heat solution that accounts for the thermal characteristics of different types of land cover in order to mitigate the UHI effect intensity (Jusuf et al., 2007; D. Lee & Oh, 2019), increase the area of green spaces, enhance water space utilization (Gunawardena et al., 2017), decrease energy consumption (Zanon & Verones, 2013), determine the relationship between green spaces and heat (Bonan, 2008; Demuzere et al., 2014; Foley et al., 2007; J.H. Kim et al., 2016; Tan et al., 2016), determine the thermal contributions of green surfaces and parking lots (Onishi et al., 2010; Takebayashi & Moriyama, 2009), and further develop urban heat-related models (Lee Chapman et al., 2007; L. Chapman & Thorne, 2006; Kusaka & Kimura, 2004a, 2004b; Masson et al., 2002). Previous research conducted on a macro- or regional scale has also examined the UHI effect considering the trade-offs between ecosystem services and urban green infrastructure (Jenerette et al., 2011; Kleerekoper et al., 2012), determined the potential heat island reduction through optimised energy consumption (Yeo et al., 2013; Zanon & Verones, 2013), assessed the impact of climate on planning policies (Schwarz et al., 2011), and developed urban greening plans (Papangelis et al., 2012). Additionally, empirical studies on a micro- or building-scale have examined the reduction in heat or heat generation based on building height and its ratio to the width along the adjacent road (H/W ratio) (Keith W. Oleson et al., 2008; Loughner et al., 2012; K. W. Oleson et al., 2011), determined the cooling effect of green roofs (D. Lee & Oh, 2019), and analysed the effects of global warming on commercial heating and cooling requirements of various building designs (Scott et al., 1994). As these studies have indicated, land cover is closely related to the thermal environment. As a result, urban zoning requirements, which dictate land cover types, should consider the thermal conditions.

1.3. Study objective and procedure

The main objective of this study was to suggest thermal zoning by identifying high-temperature regions and thermal changes within zoning districts in the city of Seoul, South Korea. Unlike previous research that measured the relationship between urban structures and heat radiation, this study focused on the improvement of the urban thermal environment and producing a map of typification by identifying Q_h distribution patterns in zoning districts using a K-means clustering analysis. To accomplish this, a method for evaluating thermal properties

in the urban area was developed to create an urban thermal zoning map that identified zoning districts with the highest Q_h . The values of Q_h were first rasterised on the zoning map based on the data detailed in Section 2.2, considering the energy budget and net radiation (Fig. 1, Appendix A and C). K-means clustering was then used to cluster the heat flux levels. The UTAs and FTAs were extracted and mapped as shown in Fig. 3. Next, the areas and mean Q_h values were calculated for each UTA and FTA (Tables 2 & 3). The identified areas were then analysed considering their constitutive ratios of five land cover types: green spaces, water surfaces, roads, impervious surfaces, and buildings (Tables A & C). The land cover composition ratios for zoning districts with UTAs (Figs. 4 & 5) and FTAs (Figs. 6 & 7) were then estimated. Finally, to establish guidelines for ensuring a comfortable thermal environment (Fig. F), the land cover ratio, building stories, building cover ratio (BCR), and floor area ratio (FAR) was analysed by comparing the UTAs with the highest Q_h with the

FTAs with the lowest Q_h (Table 4).

The results of this study are intended to contribute to the development of heat mitigation strategies based on land-use and land cover characteristics through the consideration of Q_h patterns, which quantitatively indicate the heat perceived by residents. The findings of this study could provide fundamental knowledge useful for refining and/or re-determining a thermal zoning method that considers the thermal environment in urban land-use planning.

2. Methods

2.1. Study site

Seoul has a population of nearly 10 million people living in an area of roughly 60,525 ha, resulting in a population density of 168.40 people/

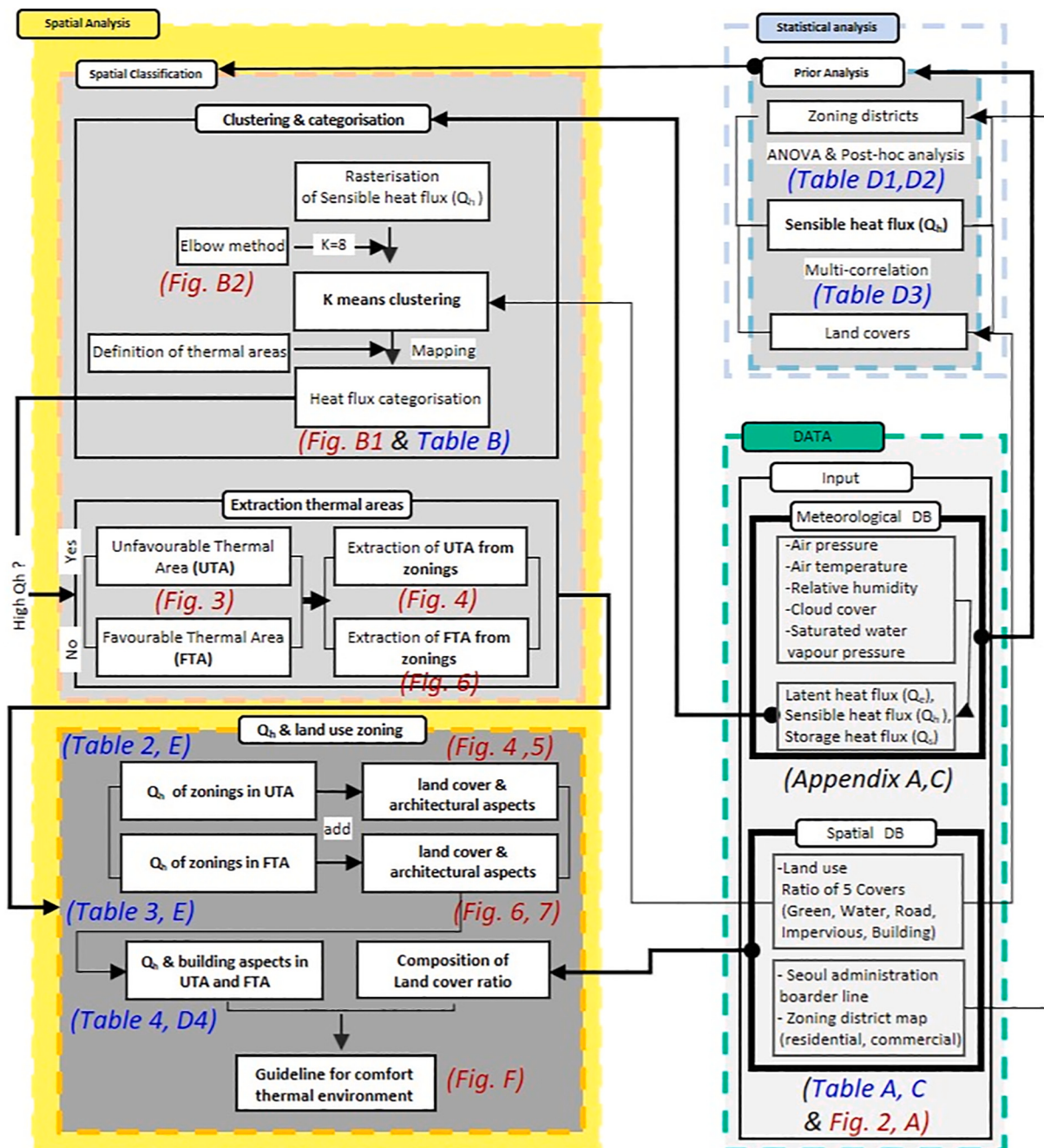


Fig. 1. Study flow.

ha (Information and Statistics Division, Ministry of the Interior and Safety, 2019). Although Seoul represents only 0.6% of the area of South Korea, it houses 19% of the total population. With 25 administrative districts, Seoul has urbanised approximately 34,420 ha of its total 60,525 ha area. These 25 districts, known as “Gu”, denote areas ranging from 1000 ha to 4700 ha. Populations in each “Gu” range from under 140,000 to 630,000. Within the “Gu”, there are 242 neighbourhood administrative districts, called “Dong”. Land-use in Seoul consists of 31.9% open green spaces, 18.9% residential areas, 13.0% mixed residential and commercial areas, 10.5% transportation facilities, 8.1% river and lake areas, 5.9% commercial areas, 5.1% for public use, and 6.6% for unknown use (C. Lee, 2013).

In terms of the natural environment, Seoul is surrounded by mountains that, combined with the waterfront areas along the Han river, affect landscape planning and present considerable issues to density management during the urban planning process (C. Lee, 2013). The W-shaped Han River flows from east to west through the middle of the city and a green belt surrounds the city. The city's geography is basin-shaped, bordered by Mt. Bukhan to the north and Mt. Gwanak to the south. The overall urban area can be divided into two parts: the southern part of the city was developed in the 1970s to improve demographic decentralisation and the northern part of the city is centred around the old town, which contains the city's historical and cultural areas as well as the central business district (CBD) (Fig. 2). As of 2000, most of the buildings built in the 1970s are considered old, leading to the ongoing

reconstruction of high-rise apartment complexes.

2.2. Data & geographic information system (GIS) methodology with zoning

To perform a thermal analysis of the study area, the average heights and coverage ratios of buildings, green space ratios, impervious surface ratios, road ratios, water surface ratios, and meteorological data, including atmospheric temperatures, atmospheric pressures, and relative humidity collected from 287 weather stations during the summer, were processed onto a 100 m resolution grid (Y.J. Kwon et al., 2018) (see Appendix A) to analyse and cluster the Q_h (see Appendix B). The high air temperature regions were then identified and the thermal changes were examined within each zoning district sub-division. The focus of our data analysis was to measure the relationship between the Q_h and the BCR and FAR in diverse land-uses including commercial, residential, and semi-industrial areas.

A zoning map was required for the heat distribution data analysis; the 2016 zoning shape file was obtained from the Seoul open database (<http://lod.seoul.go.kr/home/intro/openLod.jsp>). The shape file consisted of a 100 m resolution grid so that it could be overlaid with the shape file layer extracted from the areas with Q_h . The spatial analysis and statistics for each zone were calculated using ArcGIS 10.2 (ESRI 2014. ArcGIS Desktop: Release 10.2 Redlands, CA: Environmental Systems Research Institute). The characteristics of the processed zoning

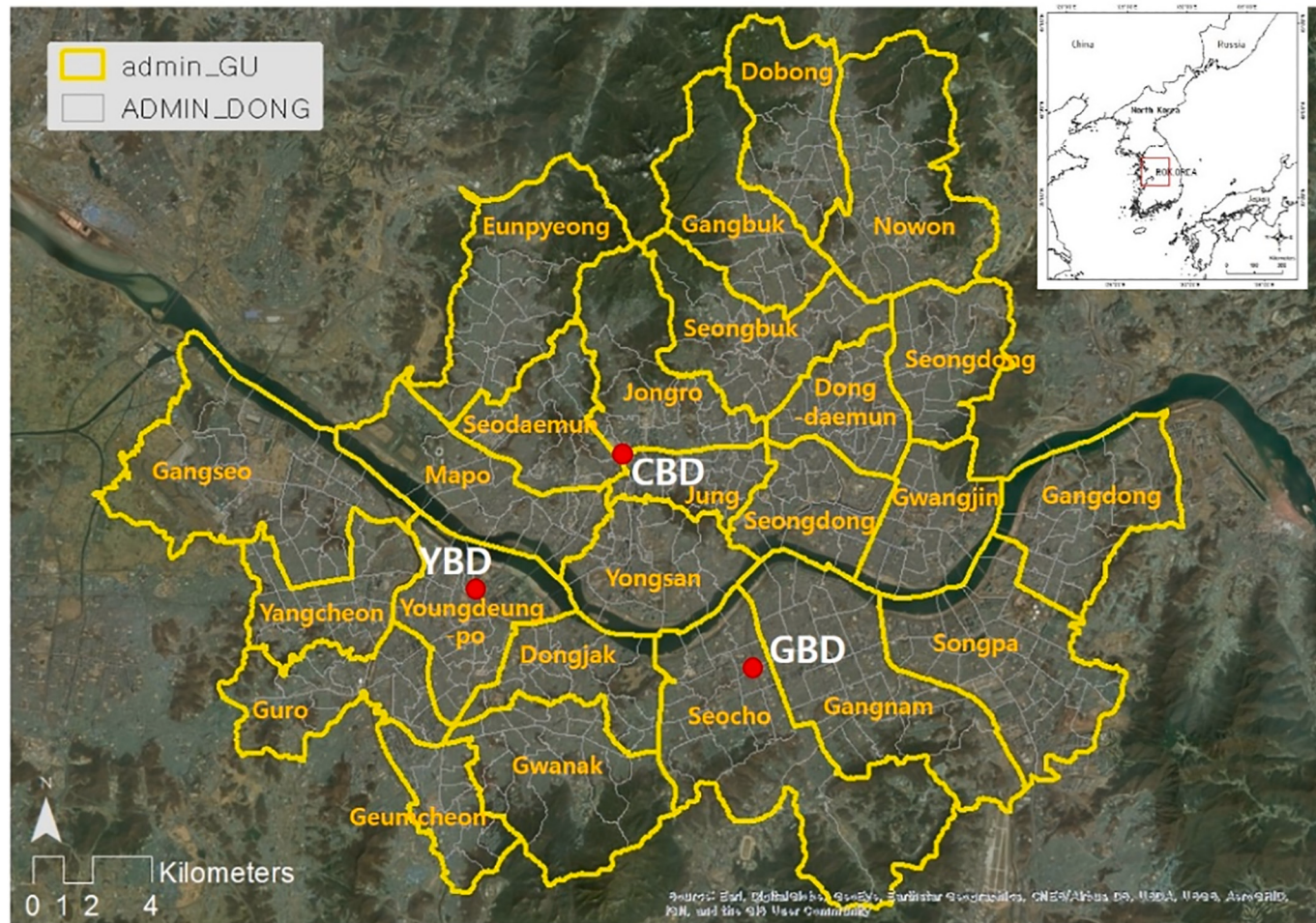


Fig. 2. CBDs in Seoul.

Note: CBD refers to a traditional business district; YBD indicates a Yeouido business district; and GBD stands for Gangnam business district. These three districts are the main urban centres in Seoul (H.M. Kim & Han, 2012). The variable “admin_GU” represents 25 administrative districts, “Gu” and “ADMIN_DONG” refers to neighbourhood administrative districts, “Dong”. Source: GIS map (<https://sgis.kostat.go.kr>).

data are as follows:

First, Korean zoning for land-use planning comprises four major zoning categories (residential, commercial, industrial, and green zones) with sixteen sub-division districts. However, there are no solely or majority industrial areas in Seoul (see Table 1). Second, the density and spatial controls provided by zoning are usually defined in terms of BCR and FAR (Gallent & Kim, 2001; Gao et al., 2006). Based on these zoning characteristics, we estimated the BCR of each zoning district by calculating the area of building-coverage corresponding to locations with Q_h (Tables 2, 3). The Q_h was estimated from the net radiation using the physical model equations and data shown in Appendix A and C. The Q_h value is known to shift based on land cover and FAR or BCR (Yang et al., 2010). As the FAR and building height are strongly related to the intensity of land-use and residents' activities (Ding, 2013) that generate heat through energy consumption, the Q_h reduction analysis was conducted by assuming that the FAR reflected both the building height and BCR.

2.3. Q_h estimation

The urban energy budget is comprised of Q_h , the latent heat flux (Q_e), and the storage heat flux (ΔQ_s) (see Appendix C). This study focuses on Q_h , which can be calculated from the net radiation (Q_n), defined as the sum of the net longwave (Q_{L^*}) and the net shortwave radiation (Q_{K^*}), and the physical equation describing the energy budget, as follows in Eq. (1) (Grimmond et al., 1991; Holtslag & van Ulden, 1983):

$$Q_n = Q_h + Q_e + \Delta Q_s \rightarrow Q_n - \Delta Q_s = Q_h + Q_e = Q_{K^*} + Q_{L^*} \quad (1)$$

The equation used to calculate Q_h (explained in detail in Appendix C) is based on empirical coefficients and a physics-based model; thus, knowing the Q_h value is more advantageous than knowing the air temperature when quantifying spatial characteristics (Y.J. Kwon et al., 2019). Moreover, the value of Q_h indicates the potential intensity of the UHI effect (Pham et al., 2019). Therefore, the distribution of Q_h can be used to devise ways of improving the urban thermal environment through zoning.

An analysis of variance (ANOVA) was run to identify the variation of multiple correlations of Q_h and the four types of zones. The ANOVA results indicate that Q_h values of the four zone types are independent of each other. Then, the Q_h was classified by zoning district. The significance of the differences among the four zone types assumed that zoning affects the change in Q_h according to the results of the post-hoc analysis (Appendix D).

2.4. K-means clustering, extracting UTA/FTA, and zoning

K-means clustering (Fig. 1) determines the mean of a spatial analysis using a statistical clustering method and can quickly cluster large quantities of data. This analysis is based on Tobler's geographical principle that what is near is more similar than what is far (Miller, 2004). The number of centripetal points in a clustered area is defined as K , which is determined by dividing the data into areas within and beyond a certain distance from the centroid of the cluster.

This study identified the zoning districts in which heat was concentrated through K-means clustering by investigating the relationship between the land-cover ratios, Q_h , and spatial characteristics of heat concentration regions using a 100 m resolution grid (Y.J. Kwon et al., 2018) (Appendix A). As in a previous study, among the 'heat-concentrated regions', Q_h in UTAs is higher than the mean value of Q_h ; similarly, Q_h in FTAs is lower than the mean value of the Q_h in the city (Y.J. Kwon et al., 2018). The UTAs and FTAs were obtained by classifying the data into eight thermal groups by K-means clustering (Appendix A and B). Then, regions with high Q_h were typified, mapped, and saved to a shape file using GIS to identify areas in which the thermal environment should be improved (Fig. B1 and Table B in the Appendix) (Y.J. Kwon et al., 2018). The areas with high Q_h concentrations (i.e., UTAs) were extracted for analysis of their corresponding zoning districts and the areas with low Q_h concentrations (FTAs) were processed in the same manner. The UTAs were determined to be locations in need of heat flux reduction, whereas the FTAs were identified as thermally comfortable areas, and the remaining areas were defined as moderate areas.

It is important to select the appropriate centroid (K) for a K-means

Table 1
BCR, FAR, green, and impervious coverage ratio in Seoul's zoning and land-use.

Zoning districts (Code)	Description	Seoul zoning area ^a		Building height (mean)	Seoul bldg. coverage ^b	Seoul FAR (CBD) ^b	Green surface ratio	Impervious surface ratio	Road ratio
		Unit	Area (ha)						
Residential									
Exclusive 1 (RE1)	Single-unit detached houses	545	0.9	10.00	0.5	1	0.58	0.23	0.09
Exclusive 2 (RE2)	Low-rise attached houses	84	0.1	10.78	0.4	1.2	0.41	0.48	0.04
General 1 (RG1)	Low-rise houses	6460	10.7	10.63	0.6	1.2	0.25	0.36	0.17
General 2 (RG2)	Mid-rise houses	13,294	21.9	16.07	0.6	2	0.15	0.37	0.20
General 3 (RG3)	High-rise houses	9418	15.5	13.60	0.6	2.5	0.16	0.41	0.21
Quasi (RQ)	Mixed use including commercial and business	1162	1.9	17.00	0.6	4	0.16	0.33	0.25
Commercial									
Neighbourhood (CN)	Providing neighbourhood service	81	0.1	15.76	0.6	6(5)	0.22	0.36	0.17
General (CG)	Commercial and business functions	2326	3.8	23.40	0.6	8(6)	0.23	0.36	0.17
Central (CC)	Central Core function in Seoul	36	0.1	29.45	0.6	10(8)	0.61	0.11	0.18
Distributional (CD)	Distribution functions for products from primary industries	156	0.3	20.10	0.6	6(5)	0.26	0.35	0.19
Industrial									
Quasi (IQ)	Light industry and mixed use	2765	4.6	9.63	0.6	4	0.34	0.01	0.15
Green									
Agricultural (GA)	Agricultural production	106	0.2	0.14	0.2	0.5	0.40	0.03	0.16
Natural (GN)	Preserved and conditionally available to develop	24,160	39.9	0.11	0.2	0.5	0.65	0.01	0.07
Preservation (GP)	Preserved area	73	0.01	0	0.2	0.5	0.95	0	0.03

^a Korean Statistical Information Service, <http://kosis.kr/> 2018.

^b Seoul building Coverage & FAR (Sung et al., 2015).

Table 2BCR, FAR, green, and impervious coverage ratio and Q_h in unfavourable thermal areas.

Zoning District Code ^a	Area	Bldg.	FAR ^b	Green	Impervious	Road	Q_h ^c	UTA	
	ha	ratio	ratio	ratio	ratio	ratio	W/m ²	ha	% ^d
CN	81	0.59	10.8	0.03	0.13	0.24	302.13±35	8	9.9
RQ	1162	0.56	3.8	0.01	0.13	0.29	301.55±33	88	7.6
CG	2326	0.57	8.4	0.04	0.15	0.23	294.92±31	92	4.0
RG1	6460	0.50	1.4	0.11	0.18	0.19	290.75±27	265	4.1
RG2	13,294	0.54	2.4	0.08	0.17	0.20	298.81±10	346	2.6
RG3	9418	0.56	2.7	0.06	0.15	0.22	291.48±23	217	2.3
RE1	545	0.27	1.0	0.20	0.34	0.17	182.52±26	3	0.6
IQ	2765	0.45	4.1	0.11	0.25	0.18	160.10±28	5	0.2
GN	24,160	0.20	0.2	0.27	0.28	0.21	160.10±22	36	0.1

^a RE2, CC, CD, GA, and GP are scattered and those of unfavourable area ratio is around 0 as ignorable values. The ratio is the number of the area per land-cover in each zoning divided by the total area of the zoning in Seoul (The sum of BCR, green, impervious, and road is close to 1.0.).

^b Most FARs in unfavourable thermal areas (UTAs) exceed the FAR regulation limits for their zoning area.

^c Range: Standard deviation of Q_h .

^d % of area = (A_i/A_t) × 100; A_i : Area of UTA or FTAs in each zoning, A_t : Total area of each zoning, Area of zoning in Seoul (Appendix Table E).

Table 3BCR, FAR, green, and impervious coverage ratio and Q_h in favourable areas.

Zoning district Code ^a	Area	Bldg.	FAR ^b	Green	Impervious	Road	Q_h ^c	FTA	
	ha	ratio	ratio	ratio	ratio	ratio	(W/m ²)	Ha	% ^d
GA	106	0.03	0.2	0.85	0.04	0.07	95.09 ± 10	10	9.50
GN	24,160	0.03	0.2	0.82	0.06	0.08	101.73 ± 27	339	1.40
RQ	1162	0.48	3.8	0.11	0.18	0.17	165.00 ± 33	16	1.38
RE1	545	0.25	0.8	0.46	0.15	0.13	104.46 ± 27	3	0.60
IQ	2765	0.35	3.9	0.25	0.17	0.15	105.47 ± 15	10	0.40
RG1	6460	0.43	1.1	0.30	0.10	0.14	156.88 ± 25	20	0.30
RG3	9418	0.47	2.3	0.22	0.12	0.17	145.72 ± 19	7	0.10
RG2	13,294	0.45	1.9	0.28	0.11	0.15	146.82 ± 29	9	0.10
CG	2326	0.51	8.4	0.23	0.08	0.17	109.86 ± 21	1	0.04

^a RE2, CN, CC, CD, and GP are scattered, and UTA ratio is around 0, an ignorable value. The ratio is the number of the area per land-cover in each zoning divided by the total area of the zoning in Seoul (The sum of BCR, green, impervious, and road is close to 1.0).

^b FARs of favourable thermal areas (FTAs) meet the FAR regulation limits for their zoning area.

^c Range: Standard deviation of Q_h .

^d % of area = ($A_i \times A_t$) × 100; A_i : Area of UTA or FTAs in each zoning, A_t : Total area of each zoning, Area of zoning (Appendix Table E).

analysis. To do so, the Calinski–Harabasz (C–H) index verification method (Mota et al., 2011; Shen et al., 2018) was applied in this study, and the distance between the clusters was calculated using the square sum of the clusters and the square sum ratio in the cluster. This result of the C–H analysis increases rapidly, indicating the number of clusters (Fig. B2 in the Appendix).

3. Results: extracting UTA/FTA with zoning

In this study, we classified the distribution of Q_h and created a map of the UTAs and FTAs in order to compute the high and low Q_h values. Regions with relatively high and low Q_h levels were compared in terms of zoning district type (Fig. 3). The ratios of UTA and FTA coverage areas over the acreage of each particular zoning district were calculated to compare the thermal environments of different zoning districts in Seoul.

3.1. Unfavourable thermal areas by zoning district

It was determined that the higher the ratio of UTAs or FTAs to the land-use area, the more the thermal environment was influenced by the zoning district type. As the UTAs indicate where heat most needs to be

dispersed, these areas should be given the highest preference in the spatial design of zoning requirements.

Nine zoning districts (abbreviations as defined in Table 1) were identified as containing UTAs: CN, RQ, CG, RG1, RG2, RG3, RE1, IQ, GN. These nine zoning districts were extracted from the initial fourteen zoning districts, excluding RE2, CC, CD, GA, and GP, which had UTA ratios of zero. The area ratios of the UTAs were derived according to land-use type in order to determine a ranking of zonings that affect the Q_h (Table 2).

As shown in Table 2, the average Q_h is highest in CN districts, with a value of 302.13 ± 35 W/m². The average ground cover composition ratios and FAR in this zoning district type were 0.03 for green spaces, 0.59 for buildings, 0.13 for impervious surfaces, 0.24 for roads, and 10.8 for FAR (Table 2). In a previous study, heat flux intensity was directly correlated to the centrality of the commercial area (Borruso & Porceddu, 2009). Also, commercial districts in the study site tend to form urban canyons (street canyons) (Hu et al., 2020) due to the substantial number of high-rise buildings, and the moving sunlit and volume of these buildings could result in a high heat flux. The smallest (non-zero) average Q_h of 160 ± 22 W/m² occurred in GN districts, which had land cover composition ratios of 0.27 for green spaces, 0.20 for buildings,

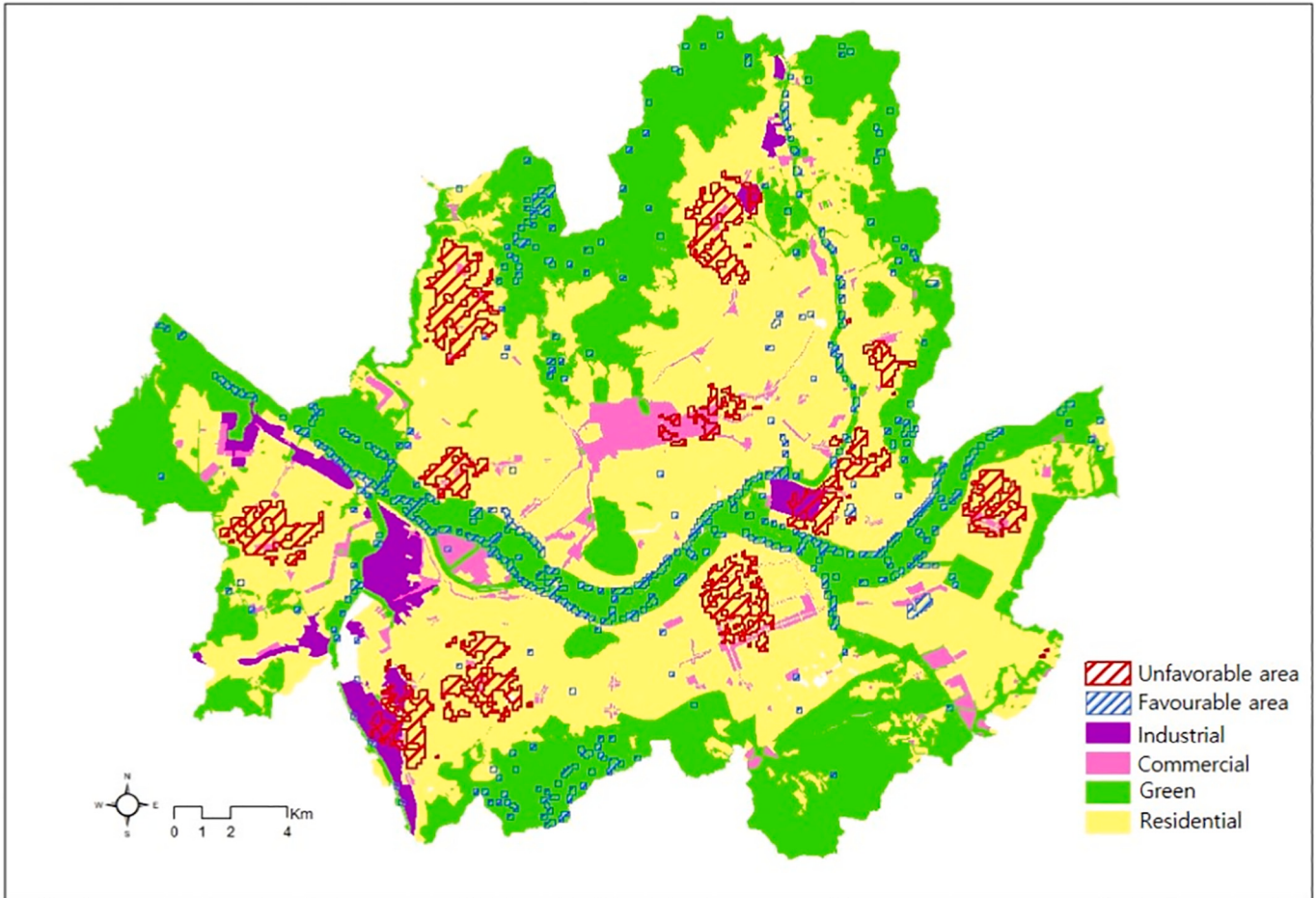


Fig. 3. Land-use zoning with UTAs and FTAs.

0.28 for impervious surfaces, 0.21 for roads, and 0.2 for FAR. Note that the reason for the relatively higher impervious surface ratio in GN is due to an existing airport categorised under a GN land-use type.

3.2. Favourable thermal areas by zoning district

A total of nine zoning districts were extracted that contained greater than 0% FTAs. Table 3 shows the FTA percentages of each of these zoning districts, arranged in descending order. The highest percentage of FTAs (9.5%) was observed for the GA zoning district, with land cover composition ratios of 0.85 for green spaces, 0.03 for buildings, 0.04 for impervious surfaces, 0.07 for roads, and 0.2 for FAR. The smallest Q_h of $95.09 \pm 10 \text{ W/m}^2$ was observed for the GA zoning district type, followed by the GN zoning district type. After these green districts, the next-lowest Q_h of $104.46 \pm 27 \text{ W/m}^2$ was observed for residential zoning district type RE1.

4. Discussion

This study investigated the distribution of sensible heat flux in Seoul using zoning to extract the UTAs and FTAs and examine factors such as FAR, BCR, and building height that affect the energy budget and thermal conditions in each type of zoning district in terms of Q_h . Clark et al. (2009) proposed that an analytical zoning map could be used during land-use planning to mitigate persistent urban warming.

4.1. Unfavourable thermal areas

It is important to determine a relative priority ranking based on total

UTAs to determine which zoning districts have the greatest influence on the UHI effect. However, due to a wide range of area coverage values for each zoning district in Seoul, the results were analysed by the percentage of UTAs located in the area of each zoning district type. This approach allowed the identification of which urban environment elements could be more effective in mitigating Q_h under similar spatial characteristics in the same size grid. Comparing the Q_h and percentage of district type occupied by UTAs in Table 2, the CN district type exhibits the highest percentage of UTAs, as well as the highest Q_h value ($302.13 \pm 35 \text{ W/m}^2$) among the nine selected zoning districts. The Q_h value is noticeably lower when the green surface ratio is higher and the BCR is lower. In contrast, for the six cases in which the BCR values are high, the Q_h values are significantly higher, as in residential and commercial districts.

Areas with a wider distribution of high Q_h likely exert a more negative effect on resident comfort than areas in which the high Q_h distribution is limited to specific, concentrated locations. The street-view images of high-UTA CN districts, shown in Fig. 4, provide examples of mixed commercial and residential zone developments in Seoul. These areas may appear similar to RQ districts, but have changed into CN districts since 2001 (Jeong, 2015). In this context, the residential area along the main roads, linear commercial districts, main commercial areas (Hong & Ahn, 2001; Jo, 2015), and shops that emerged along the street represent changes in land-use that transformed these area from RQ districts into NC districts with central business areas (Jeong, 2015). These districts therefore represent areas of mixed use that accommodate shops, housing, and neighbourhood businesses, with a high concentration of activity and expensive land prices. The concentrations of structures and impervious surfaces in these districts and the absence of green

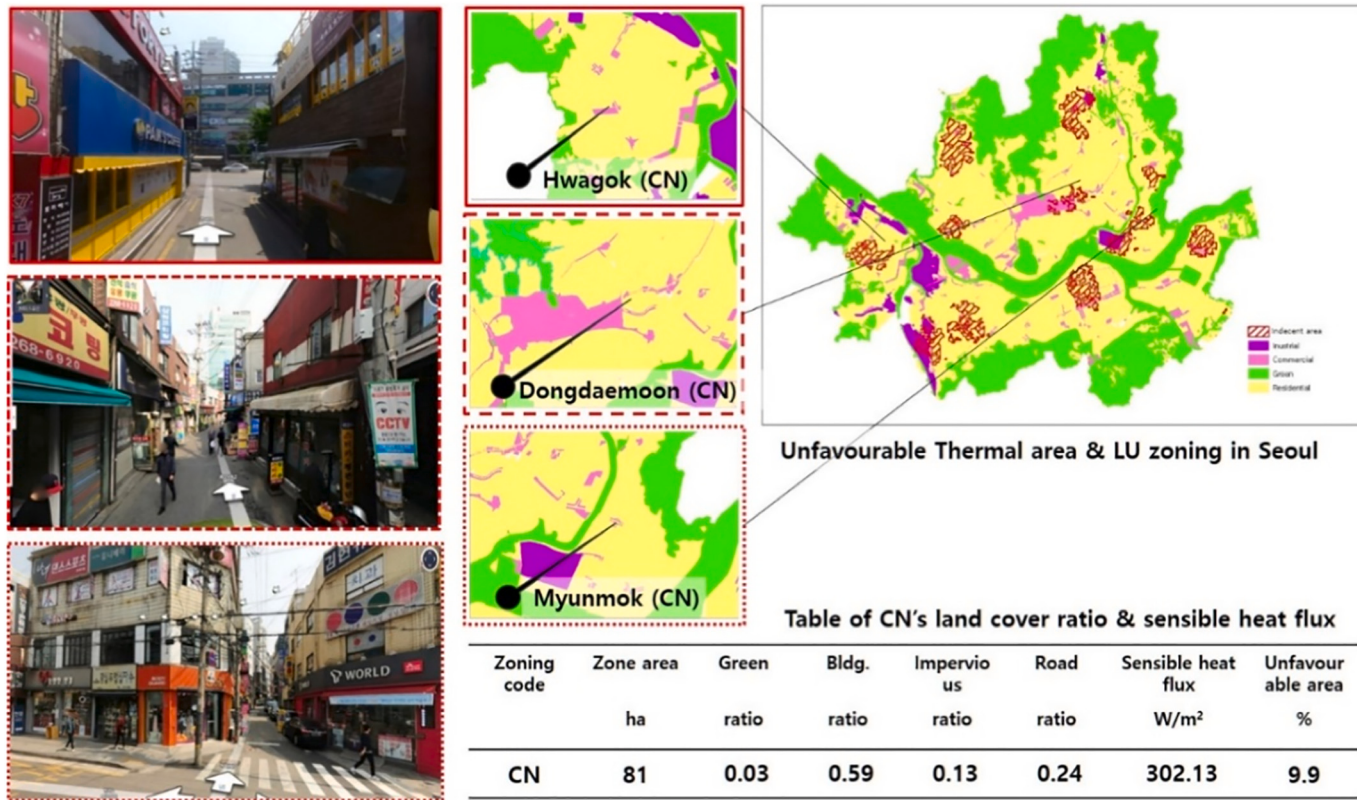


Fig. 4. UTA street view, location, and table of land cover ratio and Q_h . Photo source: <http://map.naver.com>.

space to mitigate Q_h effects (Y.J. Kwon & Lee, 2019) combine with energy sources relating to the activity inside and outside the buildings, thus affecting the total Q_h value.

Commercial districts with UTAs had an average Q_h of $\sim 298.5 \text{ W/m}^2$, while residential districts with UTAs had an average Q_h of $\sim 273.0 \text{ W/m}^2$. The BCR value was 0.55 in commercial districts and 0.53 in residential districts (Table 2, Fig. 5). The BCR was the highest of the five land cover ratios in both commercial and residential areas. Thus, the influence of BCR on the Q_h value was significant, as indicated by the observed correlation between Q_h and BCR (Table D3 in the Appendix).

Additionally, the change in BCR manifested as a similar pattern in the change in Q_h . However, the FAR values remained roughly 7.0 on average in commercial districts where the average building height was $\sim 22 \text{ m}$, and roughly 2.0 on average in residential districts where the average building height was $\sim 15 \text{ m}$. Indeed, the FAR values and building heights varied considerably according to commercial and residential districts, but BCR is not high in RE1 (Fig. 5). Therefore, the BCR was determined to be more effective than the other land cover ratios in describing the Q_h in both commercial and residential districts, while the green space land cover ratio was found to be effective in predicting the reduction of Q_h in

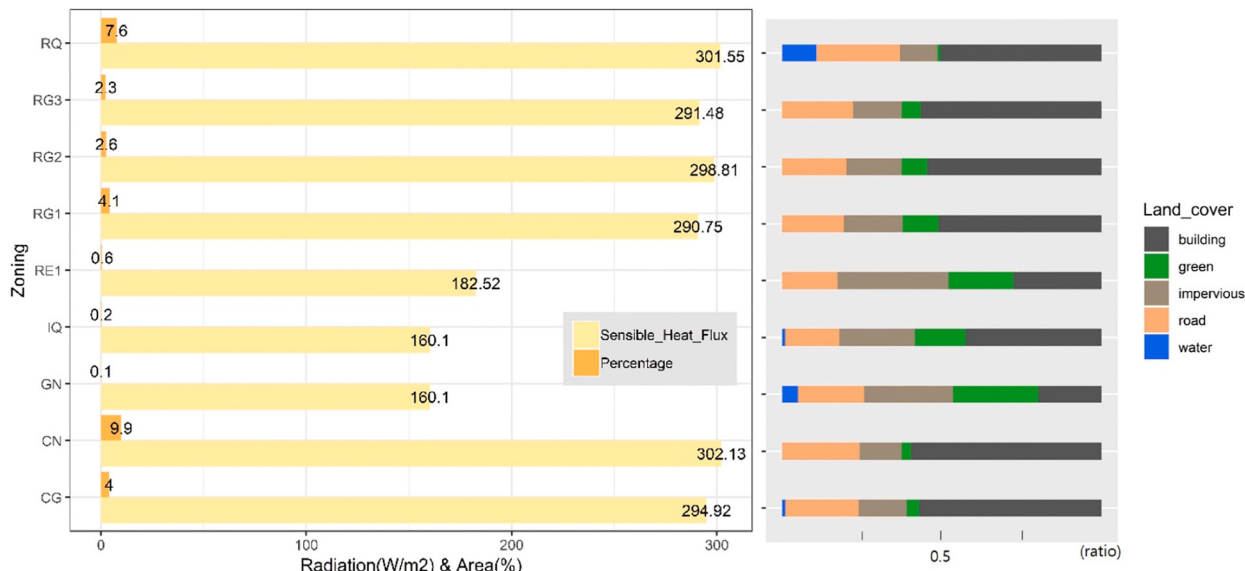


Fig. 5. Q_h and land cover ratios for unfavourable thermal areas.

residential districts.

4.2. Favourable thermal areas

The zoning districts with the lowest Q_h values in FTAs were GA and GN, which are uninhabited. Among inhabited areas of the city, zoning district RE1 had the lowest Q_h of $104.46 \pm 27 \text{ W/m}^2$. However, because the absolute area of RE1 zoning districts was relatively small, the ratio of FTAs' area in RE1 zoning districts was also quite small at 0.6% (see Table 3 & Fig. 6). The FTAs in RE1 zoning districts were mostly high-income residential areas with large plots of residential land and free-standing buildings of one to three stories.

The RE1 zoning district type is dedicated to residential use and is physically separated from commercial or other use areas (Joo & Jung, 2010). Most RE1 zoning districts consist of large amounts of green and open spaces, which absorb incoming short-wave radiation (Q_e) and convert it to Q_h , rather than buildings, which release Q_h (Fig. 7) and thus result in a low Q_h value according to the adjusted urban energy budget. As the FAR for RE1 was the lowest for all zoning districts except for the green zoning districts (Table 1), the low Q_h values in these areas are likely the result of smaller building volumes and more vegetation.

4.3. Application to zoning

Resident welfare or environmental rights are not typically considered in terms of their relationship to the thermal environment. The zoning system offers a means of land-use planning regulating FAR and BCR that can be employed to mitigate the thermal conditions (Park et al., 2018). The heat values associated with land-use and the zoning area ratios of the UTAs can be applied to improve the thermal comfort by revising or establishing new urban planning standards for basic land cover ratios (He et al., 2007), FAR, and BCR (Sriwanit & Hokao, 2012). Zoning regulations control building density by limiting the maximum volume of FAR and BCR, and according to the findings of this study,

when BCR and FAR increase, Q_h increases and the thermal environment deteriorates. Thus, the use of a designated maximum building area by limiting the BCR could help to improve urban areas thermally as it preserves a certain amount of open space in each lot (Ahsanullah & van Zandt, 2014). The findings of this study can, therefore, be used as a means of controlling and securing energy sustainability through zoning requirements and planning. Ultimately, a zoning plan that considers Q_h will save energy for more sustainable cities.

This study began by analysing the distribution of land-use zoning in areas with high Q_h concentrations, deriving the summer UTAs, then determining the cause of these high Q_h values. Based on these results, it is possible to establish a design guideline for selecting priority areas in which the energy sustainability should be enhanced. This prioritisation can be accomplished by categorising the zoning districts with UTAs according to the highest Q_h . Additionally, a method for distinguishing between UTAs and FTAs, which form the basis of thermal zoning, has been proposed in this study.

From previous studies, the heights of the buildings are related to the Q_h (Defraeye et al., 2011; Martins et al., 2016) and the average heights are related to total FAR, explaining the thermal mass (Giridharan et al., 2007). Thus, FAR should be considered for securing thermal comfort. Because the FAR values in each zoning district is different, we performed a simple linear regression analysis to measure the trend of the selected four zoning districts shown in Table 4. The regression models can capture the overall trend by considering the trends of a majority of the data points. The correlation coefficients of the regression equations are 0.84 (CN), 0.75 (CG), 0.65 (RQ), and 0.74 (RE1). The regression models related to FAR and Q_h have coefficients for FAR of 11.42 (CN), 30.40 (CG), 128.87 (RQ) and 105.03 (RE1), indicating that for a given increase in FAR, Q_h can be expected to increase by its respective coefficient for each zoning district type (Table 4). Note that CN has a lower coefficient than CG, which indicates that changes in FAR have a more considerable effect on the Q_h in CG. However, because of effect of gap between FAR regulation and current FAR, a potential range of Q_h is expected

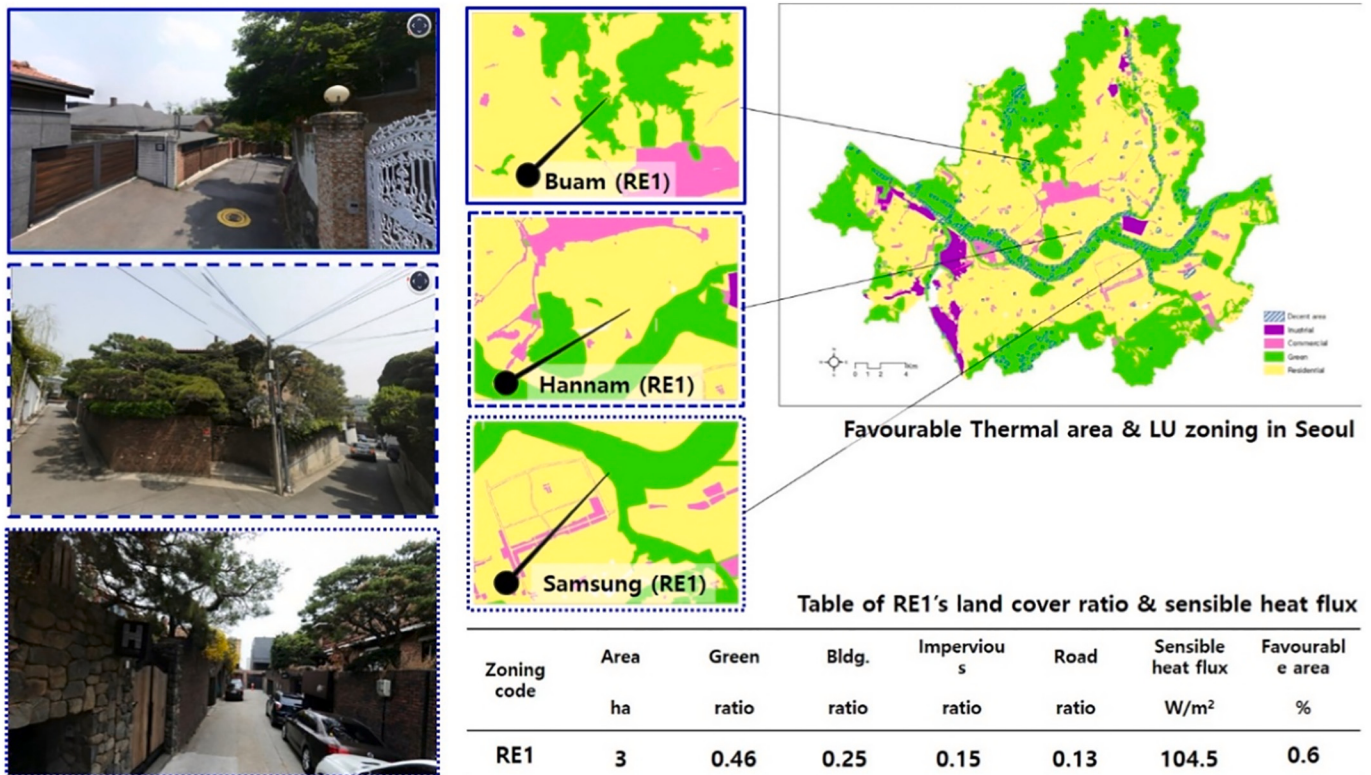


Fig. 6. FTA street view, location, and table of land cover ratio and Q_h . Photo source: <http://map.naver.com>.

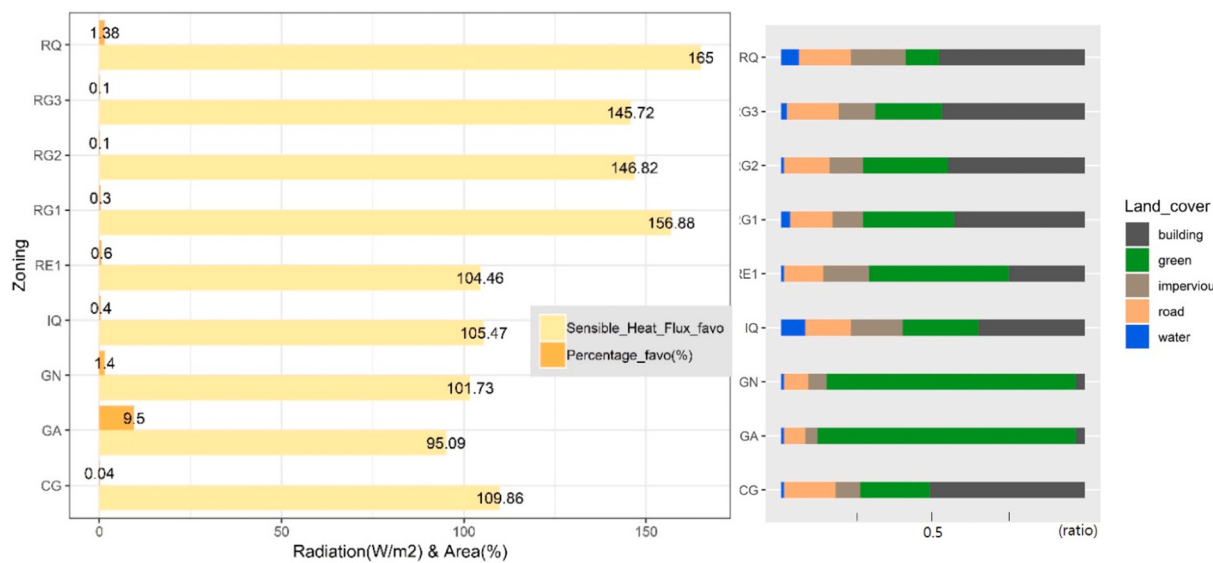
Fig. 7. Q_h and land cover ratios for favourable thermal areas.

Table 4
Comparison of CN, CG, RQ and RE1 for favourable and unfavourable areas.

Zoning district Code (Type)	Seoul FAR regulation		Current FAR		Q_h (mean) W/m ²	Regression Eq. ^b (X = FAR)	Potential range of Q_h ^d
	Ratio	Ratio	Ratio	Ratio			
Commercial							
CN (UTA)	6	10.8 ^a	0.59	302.13±35	11.42 X + 178.37 (0.84) ^c		54.8
CG (FTA)	8	8.4 ^a	0.57	109.86±21	30.40 X - 147.08 (0.75) ^c		12.2
Residential							
RQ (UTA)	4	3.8	0.48	301.55±33	128.87 X - 188.72 (0.65) ^c		25.8
RE1 (FTA)	1	0.8	0.25	104.46±27	105.03 X + 19.84 (0.74) ^c		21.0

^a There is a conciliating regulation for the FAR under exceptional condition (FAR'), FAR' = FAR X (1 + 1.2α) → α: moderate rate depending on a planning committee board (Seoul municipal ordinance Article 3. in Korean Building Act, source by <http://www.law.go.kr>).

^b Simple linear regression formula; the result of regression analysis is in Appendix Table D4.

^c Correlation coefficient of each Eq.

^d Potential range of Q_h = |{(Current FAR ratio) - (Seoul FAR regulation ratio)} × (Regression Eq. coefficient)| (unit: W/m²).

accordingly. That is why the difference between the current and regulated FAR in the CN type district is 4.8 (10.8–6 = 4.8) while the difference between the current and regulated FAR in the CG type district is 0.4 (8.4–8 = 0.4), the potential range of Q_h in CN is 54.8 W/m² due to deviations in FAR, which is greater than that of CG (12.2). On the other hand, in the case of RQ and RE1, the deviations in FAR are the same (RQ: 3.8–4 = –0.2; RE1: 0.8–1 = –0.2), but the change in Q_h is greater for RQ than for RE1 due to its larger coefficient (128.87 vs. 105.03). If the city followed the FAR regulation, the Q_h in CN and CG will be estimated around 247.33 ±35 (302.13±35–54.8) W/m² and 97.66 ±21 (109.86±21 - 12.2) W/m². Thus, the Q_h values of both commercial and residential zoning districts tend to present larger changes in UTAs due to fluctuations of the FAR.

In terms of UTAs, CN zoning districts had a BCR of 0.59 and a FAR of 10.8; whereas CG zoning districts had a BCR of 0.57 and a FAR of 8.4. This difference is the result of buildings in CN zoning districts being expanded beyond the BCR of the CG zoning districts due to different regulations implemented during the development of Seoul that permitted the construction of larger buildings in CN zoning districts. Thus, numerous small lots were collected together to construct larger buildings, causing the sizes and densities of buildings in the CN zoning districts to increase, leading to an increase in Q_h . As a result, improving

the thermal conditions in CN zoning districts should be prioritised. Our findings indicate that a large city such as Seoul needs to implement strict regulations that limit the FAR of commercial districts and closely monitor enforcement of existing FAR criteria to the greatest extent possible. Even when stakeholders demand the relief of FAR in residential districts (Yu et al., 2017), the city government must enforce the continuation of existing FAR criteria when reconstructing or redeveloping the land. Furthermore, the findings shown in Table 4 indicate that green areas could bring stronger cooling effects on the UHI effect than other types of land-use. An increase in BCR contributes to a greater increase in Q_h than any other land cover ratio (Fig. 7), whereas an increase in green cover ratio decreases Q_h more than any other land cover ratio. Although BCR is the better predictor of Q_h and therefore UTAs, the existing level of development in Seoul renders BCR regulation unrealistic. Thus, a strict enforcement of existing FAR regulations, considering the regression model in Table 4, can help ensure that adequate green areas are preserved during redevelopment to ensure comfortable thermal conditions. Although this research focused on thermal environments of a high-dense city during the summer, as a preliminary step, the findings provide a foundation for a new type of zoning that considers the thermal environment for saving energy and improving the thermal comfort. Additionally, these results can be used to formulate techniques

for mitigating high Q_h in cities expected to experience long-term effects of global warming (Corburn, 2009; J.A. Voogt, 2002). Considering UTAs in land-use planning will help to identify areas in which Q_h can be reduced by converting impervious surfaces to increase the green space ratio, for example. Moreover, this study can inform the drafting of total energy consumption regulations by identifying areas at high risk of summer energy consumption and the designation of redevelopment areas as districts in which these regulations are gradually applied.

5. Conclusions

The aim of our research is to suggest thermal zoning and show its applications to urban zoning. The basic premise of this study was that urban zoning requirements should consider the need for thermal comfort. To determine its ranges, Seoul was classified into UTAs and FTAs based on Q_h concentration in zoning districts. An analysis revealed the zoning districts containing each type of thermal area (UTA and FTA) and indicated that zoning districts with low-rise buildings and low population densities had lower levels of Q_h . In this context, Q_h can be used as a design guideline for managing the thermal environment when considering the composition of land cover (Table 4). Such considerations can also be used to review the spatial characteristics from the community street view level, minimising building cover, and planting green infrastructure in developed areas (see Fig. F in Appendix F). Finally, the BCR was found to be more effective than the other land cover ratios for predicting high Q_h in commercial and residential zoning districts, whereas green space was effective in reducing Q_h in residential districts. The results also support that improving the urban thermal environment could be achieved by adjusting the land cover ratio between green spaces, buildings, impervious cover areas, and roads, in addition to FAR, to mitigate Q_h in zoning districts.

Based on the findings, it is possible to develop and design specialised regulations for thermal zoning, applicable during the summer, that consider thermal environmental standards as zoning regulations in newly developing districts. New methods of decreasing Q_h in existing UTAs are also needed through the deployment of green infrastructure. Thermal zoning can be divided into UTAs, FTAs, and moderate areas to indicate thermal vulnerability and comfort. A legal basis should be established to temporarily apply a thermal standard of Q_h for an area, according to its thermal environment during the summer season to secure energy efficiency. Thus, thermal zoning can be used to improve thermal comfort and provide a practical motivation and means by which energy conservation can be applied during periods of elevated temperatures. Furthermore, when applied for the reduction of urban Q_h , thermal zoning can help to incentivise improved BCR and FAR enforcement by encouraging the use of green infrastructure to reduce energy consumption. The findings are useful to mitigate the UHI effect by decreasing BCR and FAR which leads to decreasing Q_h . A thermal zoning map could help planners identify areas where the UHI effect should be mitigated and therefore ensure comfortable urban spaces.

This study suggests the use of thermal zoning as a tool for urban environmental regulation as follows:

- 1) In addition to the existing functions of zoning in urban areas, zoning should also be approached from the perspective of thermal comfort, being out of only land-use efficiency.
- 2) The UTAs and FTAs in an urban area should therefore be classified according to heat concentration, using Q_h as an indicator of thermal comfort to extract optimised thermal zoning district.
- 3) Low-rise, low-population density areas will always demonstrate lower levels of Q_h , while areas with higher levels of Q_h can be

mitigated through adjustments in BCR, FAR, and green space ratios during redevelopment (Tan et al., 2016).

The proposed approach can inform appropriate energy consumption regulations and associated sustainable energy policies can indirectly contribute to a reduction in the energy usage to realise sustainable smart cities.

This study could be used to propose a seasonal zoning land-use strategy that targets energy sustainability and improved thermal comfort in the summer for urbanisation control (as per the National Land Planning and Utilization Act, Article 39) (J. Kim & Norihiro, 1998). Although this study proposes a framework for thermal zoning, it would likely be difficult to implement given that most landowners only desire zoning changes that increase their property values, which were not considered here, and indeed may not even be related to the changes proposed in this study. Despite these limitations, the thermal comfort of urban residents should be considered with the current and predicted future challenges due to the UHI effect. To face these challenges, it is necessary to develop a standard or guideline considering land cover/land-use in the urban areas by mandating a green space percentage and/or limiting the height or FAR of buildings (Appendix F). In future research, thermal regulations in land-use zoning should be developed focusing on the distribution of extreme heat and considering heat vulnerability. Accordingly, an institutional plan protecting seniors and children, who are the most vulnerable to heat, should also be developed. This research also helps to determine an optimised thermal zoning standard to mitigate the thermal environment in order to meet a target Q_h intensity range in each zoning district. A study on the winter application of thermal zoning should also be conducted by examining changes in Q_h during the winter. Finally, future research should also scrutinise the effects of urban air ventilation on Q_h .

Funding

This work was conducted with the support of the Korea Environment Industry & Technology Institute (KEITI) through its Urban Ecological Health Promotion Technology Development Project, and funded by the Korea Ministry of Environment (MOE) (2020002770003).

CRediT authorship contribution statement

You Jin Kwon: Conceptualization, Methodology, Software, Formal analysis, Data curation, Resources, Writing – original draft, Visualization, Investigation. **Dong Kun Lee:** Resources, Validation, Funding acquisition, Supervision. **Junhyun Kim:** Formal analysis, Writing - review & editing, Validation. **Kyushik Oh:** Project administration, Funding acquisition.

Declaration of competing interest

The authors declare that they have no known competing financial interests or personal relationships that could have appeared to influence the work reported in this paper.

Acknowledgments

This work was supported by the BK 21 Plus Project in 2019-2020 (Seoul National University Interdisciplinary Program in Landscape Architecture, Global Leadership Program toward Innovative Green Infrastructure). We truly appreciate the anonymous reviewers for their constructive suggestions and elaborate comments to improve the quality of this paper and also to the chief editor, P. Zhao, and other editors.

Appendix A. Input Data (Y.J. Kwon et al., 2018)

Table A

Input data and source.

Classification	Input data	Source
Meteorology data for heat flux distribution	-air temperature, -relative humidity, -cloud cover, -saturated water vapour pressure -latent heat flux Eq. -sensible flux Eq. -storage heat flux Eq.	-Korea Meteorological Administration
Thermal environment derivation to be improved	-Land cover sub-division map (green space, wetland, impervious surface) -SHP file of Seoul administrative district -Building SHP file -Road width SHP file	Holtslag & Van Ulden, 1983 Loridan & Grimmond, 2012
Spatial attributes		-Ministry of Environment, -Statistical Geographic Information Service (SGIS), -Seoul Information Communication Plaza

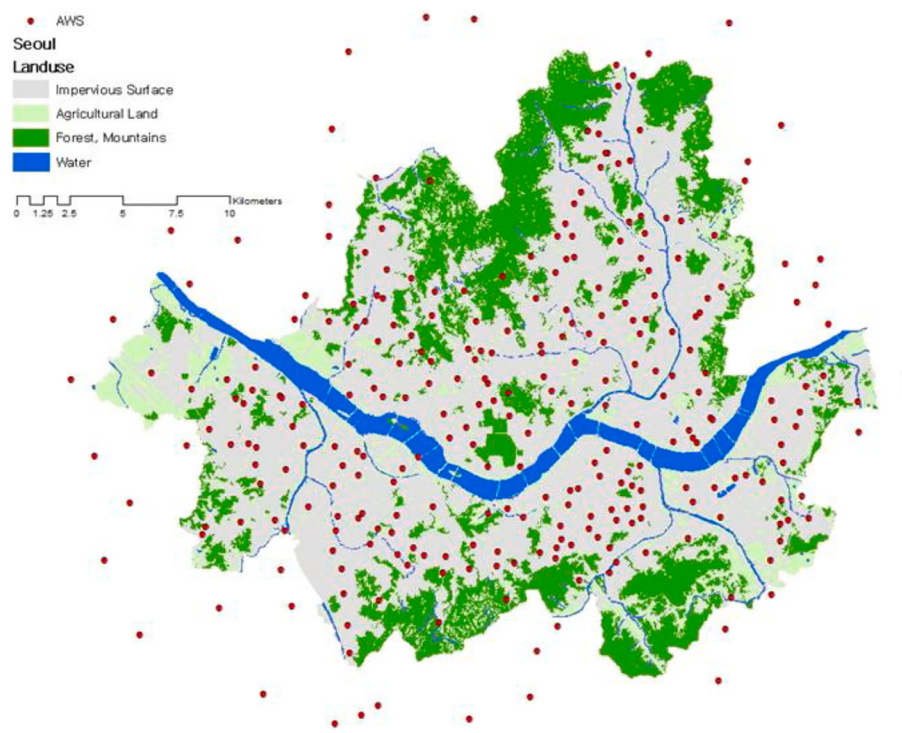


Fig. A. Automatic Weather Station (AWS) location (Y.J. Kwon et al., 2018).

Appendix B. Spatial Typification (Y.J. Kwon et al., 2018, 2019)

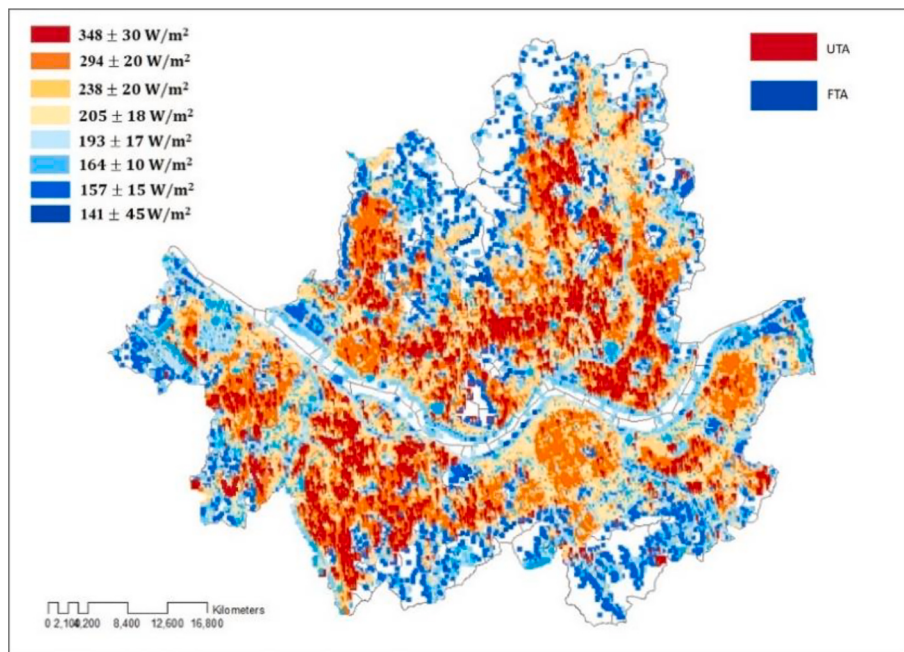


Fig. B1. Spatial typification by K-means clustering.

Table B

Eight types of thermal classification by K-means clustering (Y.J. Kwon et al., 2018).

Type	Green space	Building	Impervious surface	Wetland	Road	Latent heat	Sensible heat	Storage heat
UTA	0.03+	0.4+++	0.3++	0.0+	0.2+++	18±2	348±30	102±22
UTA	0.1++	0.2++	0.5+++	0.01+	0.2+++	21±2	294±20	195±12
UTA	0.4++	0.3++	0.2++	0.0+	0.1++	59±35	238±20	151±17
UTA	0.3++	0.1++	0.2++	0.2+++	0.2+++	62±31	205±18	189±43
FTA	0.1++	0.1++	0.7+++	0.0+	0.1++	22±5	193±17	205±38
FTA	0.4++	0.03+	0.2+	0.3+++	0.1++	103±48	164±10	168±27
FTA	0.0+	0.2++	0.5+	0.1++	0.2+++	15±3	157±15	141±25
FTA	0.8+++	0.0+	0.1+	0.02+	0.04++	109±65	141±45	76±47

+ low level, ++ middle level, +++ high level, Capital letters in “Type” column mean latent, sensible, storage heat level orderly; e.g.)

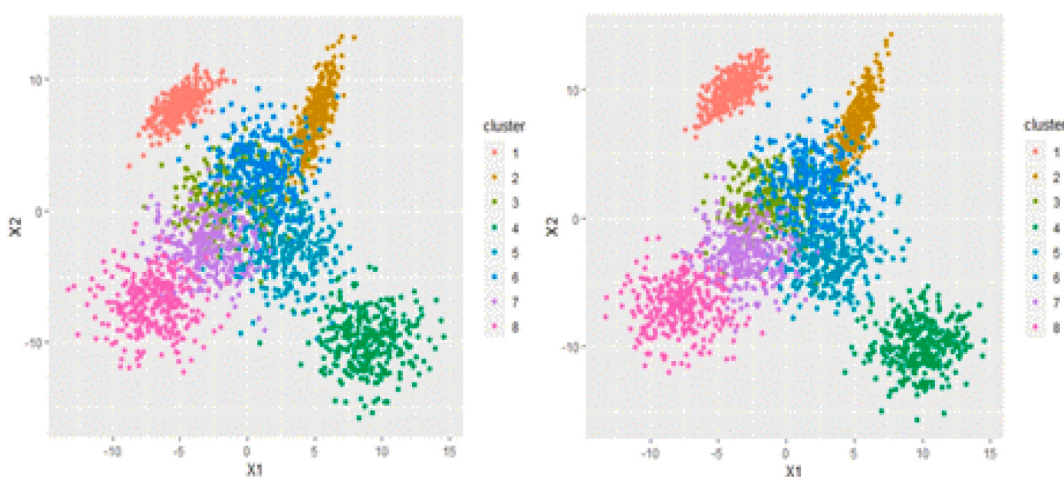


Fig. B2. Calinski-Harabasz (C—H) index analysis for testing number of K.

Calinski-Harabasz (C—H) index analysis.

$$\text{Eq. (C.1)} \quad CH(k) = \{SSB/(k - 1)\}/\{SSW/(n - k)\}$$

k: Cluster number, n: number of samples

The C—H index analysis estimates the square sum of clusters and the square sum ratio in the cluster. The result allows selecting k with the largest

value of the C—H index considering the changes of both squares.

Appendix C. Sensible heat flux estimation (Y.J. Kwon et al., 2018, 2019)

Q_n : net radiation (W/m^2)	ΔQ_s : storage heat flux (W/m^2)
Q_h : sensible heat flux (W/m^2)	Q_e : latent heat flux (W/m^2)
Q_{K^*} : net shortwave radiation (W/m^2)	Q_{L^*} : net longwave radiation (W/m^2)
f_i : land cover ratio (unitless)	a_1, a_2, a_3 : landcover coefficients
i : green cover, water cover, impervious land, building cover, and road cover (unitless)	
γ : psychrometric constant	
s : slope of the curve of saturation vapour pressure versus temperature	
α : an empirical parameter related to the moisture status of the surface	

$$\text{Eq. (A1)} \quad Q_n = Q_h + Q_e + \Delta Q_s \rightarrow Q_n - \Delta Q_s = Q_h + Q_e = Q_{K^*} + Q_{L^*} \text{ (Jackson et al., 1981)}$$

$$\text{Eq. (A2)} \quad \Delta Q_s = \sum_{i=1}^J f_i \times (a_{1i} Q_n + a_{2i} \Delta Q_s + a_{3i}) \text{ (Grimmond et al., 1991)}$$

$$\text{Eq. (A3)} \quad Q_n = [\{(1 - \alpha) + (\gamma/s)\}/\{1 + (\gamma/s)\}] \times (Q_n - \Delta Q_s) + 20 \text{ (Grimmond et al., 1991)}$$

$$\text{Eq. (A4)} \quad Q_e = \left[\alpha / \left\{ 1 + \left(\frac{\gamma}{s} \right) \right\} \right] \times (Q_n - \Delta Q_s) + 20 \text{ (Holtslag & Van Ulden, 1983)}$$

The sensible heat flux was estimated using the existing energy budget and heat flux models. The net radiation was calculated from the urban energy budget in Eq. A1, which explains the relationship between net radiation (Q_n) (and the three heat fluxes (sensible, latent, and storage heat flux) by defining the energy budget in urban areas (C.S.B. Grimmond & Oke, 2002; Jackson et al., 1981)). Next, the storage heat flux was derived from Eq. A2., which considers the empirical land cover coefficients (Table A1). Then, both the sensible heat flux and latent heat flux were estimated based on the storage heat flux (Eq. A2) as shown in Eq. A3 and Eq. A4.

Table C
Empirical land cover coefficients.

Land Cover Coefficient	a_1 (ratio)	a_2 (h)	a_3 (W/m^2)
Green	0.34	0.31	-31
Building	0.07	0.06	-5
Impervious	0.83	0.4	-54.2
Water	0.5	0.21	-39.1
Road	0.61	0.41	-27.7

Source: Grimmond and Oke (Grimmond & Oke, 2002), Roberts and Oke (Roberts et al., 2006).

Appendix D. ANOVA and Multiple Comparisons – Sensible heat flux and four types of zone

Table D1
ANOVA

qh14*	Sum of Squares	df	Mean Square	F	Sig.
Between Groups	61,009,114.4	3	20,336,371.5	6695.07	0.000
Within Groups	156,602,083.1	51,556	3037.5		
Total	217,611,197.5	51,559			

* qh14: Sensible heat flux.

Table D2
Post Hoc Analysis

Dependent Variable: qh14					
Bonferroni					
(I) class_4	(J) class_4	Mean Difference (I-J)	Std. Error	Sig.	95% Confidence Interval
100	200	-15.4876*	1.1479	0.000	-18.5161 -12.4590
	300	-4.3458*	1.1687	0.001	-7.4293 -1.2623

(continued on next page)

Table D2 (continued)

Dependent Variable: qh14						
Bonferroni						
(I) class_4	(J) class_4	Mean Difference (I-J)	Std. Error	Sig.	95% Confidence Interval	
					Lower Bound	Upper Bound
200	400	76.0348*	0.5590	0.000	74.5600	77.5095
	100	15.4876*	1.1479	0.000	12.4590	18.5161
	300	11.1418*	1.5808	0.000	6.9711	15.3125
	400	91.5223*	1.2022	0.000	88.3504	94.6943
300	100	4.3458*	1.1687	0.001	1.2623	7.4293
	200	-11.1418*	1.5808	0.000	-15.3125	-6.9711
	400	80.3806*	1.2222	0.000	77.1561	83.6051
400	100	-76.0348*	0.5590	0.000	-77.5095	-74.5600
	200	-91.5223*	1.2022	0.000	-94.6943	-88.3504
	300	-80.3806*	1.2222	0.000	-83.6051	-77.1561

*. The mean difference is significant at the 0.05 level.

100: Residential, 200: Commercial, 300: Industrial, 400: Green

An ANOVA (Table E1) and Bonferroni post-hoc analysis of Q_h and the four types of zone (Table E2) show that the difference in means among the four types of zone shows a significant difference between the classes. In other words, Q_h in each zone is different to each other so that the Q_h can be classified by the zones (Woods & Woods, 2012).

Table D3

Correlations of Sensible heat flux and five land covers (Y.J. Kwon et al., 2019).

		Q_h	gr	bd	im	Water	rd
Pearson correlation	Q_h	1.000	-0.727	0.593	0.209	-0.003	0.637
	gr	-0.727	1.000	-0.799	-0.443	0.048	-0.908
	bd	0.593	-0.799	1.000	0.542	-0.610	0.898
	im	0.209	-0.443	0.542	1.000	-0.554	0.493
	water	-0.003	0.048	-0.610	-0.554	1.000	-0.357
	rd	0.637	-0.908	0.898	0.493	-0.357	1.000
Sig. (1-tailed)	Q_h	-	0.000	0.000	0.000	0.439	0.000
	gr	0.000	-	0.000	0.000	0.003	0.000
	bd	0.000	0.000	-	0.000	0.000	0.000
	im	0.000	0.000	0.000	-	0.000	0.000
	water	0.439	0.003	0.000	0.000	-	0.000
	rd	0.000	0.000	0.000	0.000	0.000	-
N	Q_h	3240	3240	3240	3240	3240	3240
	gr	3240	3240	3240	3240	3240	3240
	bd	3240	3240	3240	3240	3240	3240
	im	3240	3240	3240	3240	3240	3240
	water	3240	3240	3240	3240	3240	3240
	rd	3240	3240	3240	3240	3240	3240

Q_h : Sensible heat flux, gr: green cover ratio, bd: building cover ratio (BCR), im: impervious cover ratio, water: water cover ratio, rd: road cover ratio

Among the five evaluated land cover types, the sensible heat flux (Q_h) has the highest correlation (-0.727) with green spaces, but green spaces negatively affect Q_h . We found that the BCR and road cover ratio correlate with Q_h , but that impervious surfaces and water surfaces do not. This is because the absolute ratios of impervious surfaces and water surfaces are equivalent to small portions of the overall land surface in Seoul.

Table D4

Simple linear regression analysis of CN, CG, RQ and RE1.

	Coef.	Std err	t	P	[0.025	0.975]	R ²
Const.	178.3694	10.82595	16.47609	1.52E-23	156.6989	200.0399	
CN	11.41915	0.971334	11.75616	5.52E-17	9.474813	13.36348	0.839282
Const.	-147.079	33.33924	-4.41158	6.14E-05	-214.187	-79.9703	
CG	30.39943	3.962892	7.671021	9.07E-10	22.42254	38.37632	0.74917
Const.	-188.71790	67.55117	-2.7937	0.00705	-323.936	-53.4995	
RQ	128.87399	17.94992	7.179642	1.46E-09	92.94333	164.8047	0.653043
Const.	19.84044	11.60484	1.709669	0.094066	-3.51889	43.19977	
RE1	105.0336	13.95744	7.525277	1.49E-09	76.93871	133.1284	0.738473

In the output above, we can see that the variables of Q_h are significant because their p-values are under 0.001.

Appendix E. Zoning in Seoul

Table E
unit (km^2).

	Exclusive	1st-type	5		Central	0.4
		2nd-type	0.7		General	22.6
		1st-type	67		Neighbourhood	0.8
Residential	General	2nd-type (under 7 stories)	86		Distributional	1.5
		2nd-type (over 7 stories)	55		Quasi-industrial	20
		3rd-type	99		Agricultural	1
	Quasi	Quasi	13.1		Natural	233.3
					Preservation	0.1

Source: Seoul Statistics, 2018

Appendix F. Street views of thermal unfavourable and favourable areas

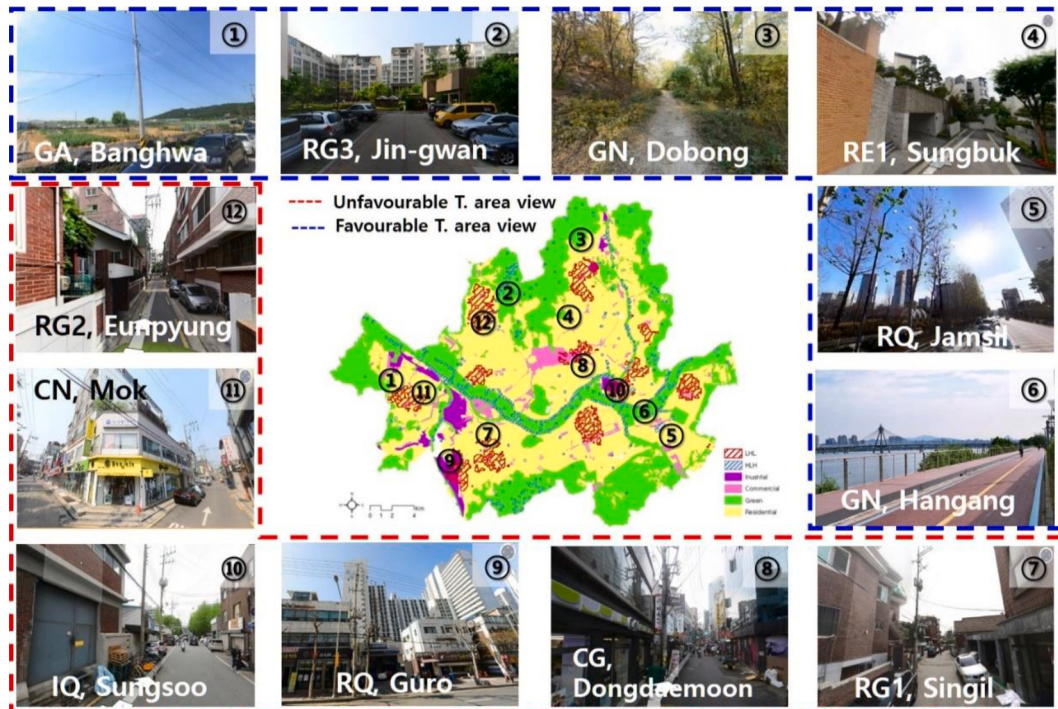


Fig. F. Street views of UTAs and FTAs.

Street views of FTAs (in box with blue dotted line): ① Agricultural green, ② 3rd-type General residential, ③ Natural green (mountain), ④ 1st-type Exclusive residential, ⑤ Quasi-residential, ⑥ Natural green (river); Street views of UTAs (in box with red dotted line): ⑦ 1st-type General residential, ⑧ General commercial, ⑨ Quasi-residential, ⑩ Industrial, ⑪ Neighbourhood commercial, ⑫ 2nd-type General residential.

References

- Acero, J. A., Arrizabalaga, J., Kupski, S., & Katschner, L. (2013). Deriving an Urban Climate Map in coastal areas with complex terrain in the Basque Country (Spain). *Urban Climate*, 4, 35–60. <https://doi.org/10.1016/j.uclim.2013.02.002>.
- Ahsanullah, S. I., & Van Zandt, S. (2014). The impact of zoning regulations on thermal comfort in non-conditioned housing in hot, humid climates: Findings from Dhaka, Bangladesh. *Journal of Housing and the Built Environment*, 29(4), 677–697. <https://doi.org/10.1007/s10901-013-9373-2>.
- Baker, L. A., Brazel, A. J., Selover, N., Martin, C., McIntyre, N., Steiner, F. R., ... Musacchio, L. (2002). Urbanization and warming of Phoenix (Arizona, USA): Impacts, feedbacks and mitigation. *Urban Ecosystem*, 6(3), 183–203. <https://doi.org/10.1023/A:1026101528700>.
- Baum, S., Yigitcanlar, T., Horton, S., Velibeyoglu, K., & Gleeson, B. (2007). Knowledge work(ers) in urban context. In *The role of community and lifestyle in the making of a knowledge city* (pp. 18–24). Retrieved from <http://scholar.google.com/scholar?hl=en&btnG=Search&q=intitle:The+Role+of+Community+and+Lifestyle+in+the+Making+of+a+Knowledge+City#0>.
- Bonan, G. B. (2008). Forests and climate change : Climate benefits of forests. *Science*, 320 (June), 1444–1449.
- Borruso, G., & Porceddu, A. (2009). *A tale of two cities: Density analysis of CBD on two midsize urban areas in northeastern Italy*. Berlin, Heidelberg: Springer.
- Buffel, T., & Phillipson, C. (2016). Can global cities be ‘age-friendly cities’ ? Urban development and ageing populations. *JCIT*, 55, 94–100. <https://doi.org/10.1016/j.cities.2016.03.016>.
- Chan, E. H. W., & Lee, G. K. L. (2009). Design considerations for environmental sustainability in high density development: A case study of Hong Kong. *Environment, Development and Sustainability*, 11(2), 359–374. <https://doi.org/10.1007/s10668-007-9117-0>.
- Chapman, L., & Thornes, J. E. (2006). A geomatics-based road surface temperature prediction model. *Science of the Total Environment*, 360(1–3), 68–80. <https://doi.org/10.1016/j.scitotenv.2005.08.025>.
- Chapman, L., Thornes, J. E., & Bradley, A. V. (2007). Modelling of road surface temperature from a geographical parameter database. Part 2: Numerical. *Meteorological Applications*, 8(4), 421–436. <https://doi.org/10.1017/s1350482701004042>.
- Clark, J. K., McChesney, R., Munroe, D. K., & Irwin, E. G. (2009). Spatial characteristics of exurban settlement pattern in the United States. *Landscape and Urban Planning*, 90 (3–4), 178–188. <https://doi.org/10.1016/j.landurbplan.2008.11.002>.
- Corburn, J. (2009). Cities, climate change and urban heat island mitigation: Localising global environmental science. *Urban Studies*, 46(2), 413–427. <https://doi.org/10.1177/0042098008099361>.
- Coutts, A. M., Beringer, J., & Tapper, N. J. (2007). Impact of increasing urban density on local climate: Spatial and temporal variations in the surface energy balance in Melbourne, Australia. *Journal of Applied Meteorology and Climatology*, 46(4), 477–493. <https://doi.org/10.1175/JAM2462.1>.

- Dear, M., & Scott, A. J. (1981). In M. Dear, & Scott (Eds.), *Urbanization and urban planning in capitalist society*. <https://doi.org/10.4324/9781351068000>.
- Defraeye, T., Blocken, B., & Carmeliet, J. (2011). Convective heat transfer coefficients for exterior building surfaces: Existing correlations and CFD modelling. *Energy Conversion and Management*, 52(1), 512–522. <https://doi.org/10.1016/j.enconman.2010.07.026>.
- Demuzere, M., Orru, K., Heidrich, O., Olazabal, E., Geneletti, D., Orru, H., ... Faehnle, M. (2014). Mitigating and adapting to climate change: Multi-functional and multi-scale assessment of green urban infrastructure. *Journal of Environmental Management*, 146, 107–115. <https://doi.org/10.1016/j.jenvman.2014.07.025>.
- Ding, C. (2013). Building height restrictions, land development and economic costs. *Land Use Policy*, 30(1), 485–495. <https://doi.org/10.1016/j.landusepol.2012.04.016>.
- Fischel, W. A. (1999). *2200 Zoning and land use regulation* (Vol. 469).
- Foley, J. A., Costa, M. H., Delire, C., Ramankutty, N., & Snyder, P. (2007). Green surprise? How terrestrial ecosystems could affect earth's climate. *Frontiers in Ecology and the Environment*, 1(1), 38–44. [https://doi.org/10.1890/1540-9295\(2003\)001_0038:gshtec2.0.co;2](https://doi.org/10.1890/1540-9295(2003)001_0038:gshtec2.0.co;2).
- Gallent, N., & Kim, K. S. (2001). Land zoning and local discretion in the Korean planning system. *Land Use Policy*, 18(3), 233–243. [https://doi.org/10.1016/S0264-8377\(01\)00017-5](https://doi.org/10.1016/S0264-8377(01)00017-5).
- Gao, X., Asami, Y., & Katsumata, W. (2006). Evaluating land-use restrictions concerning the floor area ratio of lots. *Environment and Planning C: Government and Policy*, 24(4), 515–532. <https://doi.org/10.1068/c0531>.
- Giridharan, R., Lau, S. S. Y., Ganeshan, S., & Givoni, B. (2007). Urban design factors influencing heat island intensity in high-rise high-density environments of Hong Kong. *Building and Environment*, 42(10), 3669–3684. <https://doi.org/10.1016/j.buildenv.2006.09.011>.
- Gowdy, J. (2005). Toward a new welfare economics for sustainability. *Ecological Economics*, 53(2), 211–222. <https://doi.org/10.1016/j.ecolecon.2004.08.007>.
- Grimm, N. B., Faeth, S. H., Golubiewski, N. E., Redman, C. L., Wu, J., Bai, X., & Briggs, J. M. (2015). *Global change and the ecology of cities SUPPLEMENTARY*. 319 (5864) pp. 756–760. <https://doi.org/10.1126/science.1150195>.
- Grimmond, C. S. B., Cleugh, H. A., & Oke, T. R. (1991). An objective urban heat storage model and its comparison with other schemes. *Atmospheric Environment. Part B. Urban Atmosphere*, 25(3), 311–326. [https://doi.org/10.1016/0957-1272\(91\)90003-W](https://doi.org/10.1016/0957-1272(91)90003-W).
- Grimmond, C. S. B., & Oke, T. R. (2002). Turbulent heat fluxes in urban areas: Observations and a local-scale urban meteorological parameterization scheme (LUMPS). *Journal of Applied Meteorology*, 41(7), 792–810. [https://doi.org/10.1175/1520-0450\(2002\)041<0792:THFLUA>2.0.CO;2](https://doi.org/10.1175/1520-0450(2002)041<0792:THFLUA>2.0.CO;2).
- Grossi, G., & Pianezzi, D. (2017). *Smart cities: Utopia or neoliberal ideology?* 69(December 2016) pp. 79–85. <https://doi.org/10.1016/j.cities.2017.07.012>.
- Gunawardena, K. R., Wells, M. J., & Kershaw, T. (2017). Utilising green and bluespace to mitigate urban heat island intensity. *Science of the Total Environment*, 584–585, 1040–1055. <https://doi.org/10.1016/j.scitotenv.2017.01.158>.
- Halleux, J. M., Marcinczak, S., & van der Krabben, E. (2012). The adaptive efficiency of land use planning measured by the control of urban sprawl. The cases of the Netherlands, Belgium and Poland. *Land Use Policy*, 29(4), 887–898. <https://doi.org/10.1016/j.landusepol.2012.01.008>.
- Gyurko, Joseph, Saiz, Albert, & Summers, Anita (2008). A new measure of the local regulatory environment for housing markets: The Wharton residential land use regulatory index. *Urban Studies*, 45(3), 693–729. <https://doi.org/10.1177/0042098007087341>.
- He, J. F., Liu, J. Y., Zhuang, D. F., Zhang, W., & Liu, M. L. (2007). Assessing the effect of land use/land cover change on the change of urban heat island intensity. *Theoretical and Applied Climatology*, 90(3–4), 217–226. <https://doi.org/10.1007/s00704-006-0273-1>.
- Holtslag, A. A. M., & Van Ulden, A. P. (1983). A simple scheme for daytime estimates of the surface fluxes from routine weather data. *Journal of Climate and Applied Meteorology*, 22(4), 517–529. <https://doi.org/10.1175/1520-0450>.
- Hong, K., & Ahn, K. (2001). A study on the relationship between the urban fabric and the architectural forms of linear commercial districts. *Journal of the Architectural Institute of Korea Planning & Design*, 17(1), 103–111.
- Hu, C. B., Zhang, F., Gong, F. Y., Ratti, C., & Li, X. (2020). Classification and mapping of urban canyon geometry using Google Street View images and deep multitask learning. *Building and Environment*, 167(September 2019), 106424. <https://doi.org/10.1016/j.buildenv.2019.106424>.
- Information and Statistics Division, Ministry of the Interior and Safety. (2019). Administrative division, 21. *Statistical Yearbook of MOIS* (p. 10). Ministry of the Interior and Safety.
- Jackson, R. D., Idso, S. B., Reginato, R. J., & Pinter, P. J. (1981). Canopy temperature as a crop water stress indicator. *Water Resources Research*, 17(4), 1133–1138. <https://doi.org/10.1029/WR017i004p01133>.
- Jenerette, D. G., Harlan, S. L., Stefanov, W. L., & Martin, C. A. (2011). Ecosystem services and urban heat riskscape moderation: Water, green spaces, and social inequality in Phoenix, USA. *Ecological Applications*, 21(7), 2637–2651. Retrieved from <http://www.esajournals.org/doi/pdf/10.1890/10-1493.1%5Cnhttp://ovidsp.ovid.co/m/ovidweb.cgi?T=JS&PAGE=reference&D=emed10&NEWS=N&AN=22073649>.
- Jeong, H. (2015). Suggestions for the introduction of localized land use zones in Seoul. Retrieved from <http://www.dbpia.co.kr/Article/NODE06338836>.
- Jiang, L., & O'Neill, B. C. (2017). Global urbanization projections for the shared socioeconomic pathways. *Global Environmental Change*, 42, 193–199. <https://doi.org/10.1016/j.gloenvcha.2015.03.008>.
- Jo, A. (2015). *Spatial pattern of commercial uses in residential zoning districts in Seoul*. Seoul national university.
- Joo, Y. S., & Jung, S. Y. (2010). A study on the solution to improve density control methods of residential areas. *Journal of the Korean Cadastre Information Association*, 12(1), 173–185.
- Jusuf, S. K., Wong, N. H., Hagen, E., Anggoro, R., & Hong, Y. (2007). The influence of land use on the urban heat island in Singapore. *Habitat International*, 31(2), 232–242. <https://doi.org/10.1016/j.habitatint.2007.02.006>.
- Kim, H. M., & Han, S. S. (2012). Seoul. *Cities*, 29(2), 142–154. <https://doi.org/10.1016/j.cities.2011.02.003>.
- Kim, I., Lee, J., Yang, J., Jang, N., Ko, J., & Jeong, B. (2013). *2030 Seoul Master Plan* (Vol. 1). Retrieved from http://urban.seoul.go.kr/4DUPIS/download/sub3_1/3_re_report.pdf.
- Kim, J., & Norihiro, N. (1998). A comparative study on the principles and the development controls of urban containment programs in UK, Japan, U.S, and Korea. *Journal of Korea Planning Association*, 33(3), 63–78.
- Kim, J. H., Gu, D., Sohn, W., Kil, S. H., Kim, H., & Lee, D. K. (2016). Neighborhood landscape spatial patterns and land surface temperature: An empirical study on single-family residential areas in Austin, Texas. *International Journal of Environmental Research and Public Health*, 13(9). <https://doi.org/10.3390/ijerph13090880>.
- Kleereker, L., Van Esch, M., & Salcedo, T. B. (2012). How to make a city climate-proof, addressing the urban heat island effect. *Resources, Conservation and Recycling*, 64, 30–38. <https://doi.org/10.1016/j.resconrec.2011.06.004>.
- Kusaka, H., & Kimura, F. (2004a). Coupling a single-layer urban canopy model with a simple atmospheric model: Impact on urban Heat Island simulation for an idealized case. *Journal of the Meteorological Society of Japan*, 82(1), 67–80. <https://doi.org/10.2151/jmsj.82.67>.
- Kusaka, Hiroyuki, & Kimura, Fujio (2004b). Thermal effects of urban canyon structure on the nocturnal heat island: Numerical experiment using a mesoscale model coupled with an urban canopy model. *Journal of Applied Meteorology*, 43(12), 1899–1910. <https://doi.org/10.1175/JAM2169.1>.
- Kwon, Y. J., Ahn, S., Lee, D. K., Yoon, E. J., Sung, S., & Lee, K. (2018). Spatial Typification based on heat balance for improving thermal environment in Seoul. *Journal of Korea Planning Association*, 53(7), 109–126. <https://doi.org/10.14249/eia.2019.28.1.23>.
- Kwon, Y. J., & Lee, D. K. (2019). Thermal comfort and longwave radiation over time in urban residential complexes. *Sustainability*, 11(8), 2251. <https://doi.org/10.3390/su11082251>.
- Kwon, Y. J., Lee, D. K., & Kwon, Y. H. (2020). Is sensible heat flux useful for the assessment of thermal vulnerability in Seoul (Korea)? *International Journal of Environmental Research and Public Health*, 17(3). <https://doi.org/10.3390/ijerph17030963>.
- Kwon, Y. J., Lee, D. K., & Lee, K. (2019). Determining favourable and unfavourable thermal areas in Seoul using in-situ measurements: A preliminary step towards developing a smart city. *Energies*, 12(2320), 1–24. <https://doi.org/10.3390/3n121222320>.
- Lai, L. W. C. (1994). The economics of land-use zoning: A literature review and analysis of the work of coase. *Town Planning Review*, 65(1), 77–98.
- Lee, C. (S. I. (2013). Geographical Atlas of Seoul 2013. Retrieved from [http://data.si.re.kr/sites/default/files/file/지도로본서울2013\(9장_토지이용\).pdf](http://data.si.re.kr/sites/default/files/file/지도로본서울2013(9장_토지이용).pdf).
- Lee, D., & Oh, K. (2019). Developing the urban thermal environment management and planning (UTEMP) system to support urban planning and design. *Sustainability (Switzerland)*, 11(8). <https://doi.org/10.3390/su11082224>.
- Loridan, T., & Grimmond, C. S. B. (2012). Characterization of energy flux partitioning in urban environments: Links with surface seasonal properties. *Journal of Applied Meteorology and Climatology*, 51(2), 219–241. <https://doi.org/10.1175/JAMC-D-11-038.1>.
- Loughner, C. P., Allen, D. J., Zhang, D. L., Pickering, K. E., Dickerson, R. R., & Landry, L. (2012). Roles of urban tree canopy and buildings in urban heat island effects: Parameterization and preliminary results. *Journal of Applied Meteorology and Climatology*, 51(10), 1775–1793. <https://doi.org/10.1175/JAMC-D-11-0228.1>.
- Martins, T. A. de L., Adolphe, L., Bastos, L. E. G., & Martins, M. A. de L. (2016). Sensitivity analysis of urban morphology factors regarding solar energy potential of buildings in a Brazilian tropical context. *Solar Energy*, 137, 11–24. doi:<https://doi.org/10.1016/j.solener.2016.07.053>.
- Masson, V., Grimmond, C. S. B., & Oke, T. R. (2002). Evaluation of the town energy balance (TEB) scheme with direct measurements from dry districts in two cities. *Journal of Applied Meteorology*, 41(10), 1011–1026. <https://doi.org/10.1175/1520-0450.2002.0450.0001>.
- Mclaughlin, R. B. (2012). Land use regulation: Where have we been, where are we going? *Cities*, 29, S50–S55. <https://doi.org/10.1016/j.cities.2011.12.002>.
- Miller, H. J. (2004). Tobler's first law and spatial analysis. *Annals of the Association of American Geographers*, 94(2), 284–289. <https://doi.org/10.1111/j.1467-8306.2004.09402005.x>.
- Mixon, J., & Dougherty, J. L. J. (1999). Texas municipal zoning law. In LexisNexis (3rd ed.) Retrieved from <https://store.lexisnexis.com/products/texas-municipal-zoning-law-skus/Sku7158>.
- Mota, S., García, M. O., Rocha, A., & Pérez-Fontán, F. (2011). Clustering of the multipath radio channel parameters. In *Proceedings of the 5th European Conference on Antennas and Propagation (EUCAP)* (pp. 3232–3236).
- Neirotti, P., De Marco, A., Cagliano, A. C., Mangano, G., & Scorrano, F. (2014). Current trends in Smart City initiatives : Some stylized facts. *Cities*, 38, 25–36. <https://doi.org/10.1016/j.cities.2013.12.010>.
- Németh, J., & Langhorst, J. (2014). *Rethinking urban transformation: Temporary uses for vacant land*. 40 pp. 143–150. <https://doi.org/10.1016/j.cities.2013.04.007>.
- Norton, B. (2007). Sustainability, human welfare and ecosystem health. *Environmental Values*, 1(2), 97–111. <https://doi.org/10.3197/096327192776680133>.

- Oleson, K. W., Bonan, G. B., Feddema, J., & Jackson, T. (2011). An examination of urban heat island characteristics in a global climate model. *International Journal of Climatology*, 31(12), 1848–1865. <https://doi.org/10.1002/joc.2201>.
- Oleson, K. W., Bonan, B., Feddema, J., Vertenstein, M., & Grimmond, C. S. B. (2008). An urban parameterization for a global climate model. Part 1: Formulation and evaluation for two cities. *Journal of Applied Meteorology and Climatology*, 47(4), 1038–1060. <https://doi.org/10.1175/2007JAMC1597.1>.
- Onishi, A., Cao, X., Ito, T., Shi, F., & Imura, H. (2010). Evaluating the potential for urban heat-island mitigation by greening parking lots. *Urban Forestry and Urban Greening*, 9 (4), 323–332. <https://doi.org/10.1016/j.ufug.2010.06.002>.
- Outubu, A. K. (1992). Land use zoning in a changing urban environment. *Contemporary Issues in Law*, 1–28.
- Papangelis, G., Tombrou, M., Dandou, A., & Kontos, T. (2012). An urban “green planning” approach utilizing the Weather Research and Forecasting (WRF) modeling system. A case study of Athens, Greece. *Landscape and Urban Planning*, 105(1–2), 174–183. <https://doi.org/10.1016/j.landurbplan.2011.12.014>.
- Park, B., Oh, K., Hanyang, U., & Hong, S. (2018). Analysis of the changes in urban thermal environments considering development densities. *International Journal of Environmental Science and Development*, 9(2), 32–37.
- Pham, J. V., Baniassadi, A., Brown, K. E., Heusinger, J., & Sailor, D. J. (2019). Comparing photovoltaic and reflective shade surfaces in the urban environment: Effects on surface sensible heat flux and pedestrian thermal comfort. *Urban Climate*, 29 (January). <https://doi.org/10.1016/j.uclim.2019.100500>.
- Pogodzinski, J. M., & Sass, T. R. (2017). The Economic Theory of Zoning: A Critical Review Author(s): J. Michael Pogodzinski and Tim R. Sass Source: Land Economics, Vol. 66, No. 3, Private Markets, Public Decisions: An Assessment of Local Land-Use Controls for the 1990s (Aug., 199, 66(3), 294–314.
- Ramaswami, A., Russell, A. G., Culligan, P. J., Rahul Sharma, K., & Kumar, E. (2016). Meta-principles for developing smart, sustainable, and healthy cities. *Science*, 352 (6288), 940–943. <https://doi.org/10.1126/science.aaf7160>.
- Roberts, S. M., Oke, T. R., Grimmond, C. S. B., & Voogt, J. A. (2006). Comparison of four methods to estimate urban heat storage. *Journal of Applied Meteorology and Climatology*, 45(12), 1766–1781. <https://doi.org/10.1175/JAM2432.1>.
- Roweis, S. T., & Scott, A. J. (1981). The urban land question *. In M. Dear, & A. J. Scott (Eds.), *Urbanization and urban planning in capitalist society* (pp. 123–158). <https://doi.org/10.4324/9781351068000>.
- Schwarz, N., Bauer, A., & Haase, D. (2011). Assessing climate impacts of planning policies—an estimation for the urban region of Leipzig (Germany). *Environmental Impact Assessment Review*, 31(2), 97–111. <https://doi.org/10.1016/j.eiar.2010.02.002>.
- Scott, M. J., Wrench, L. E., & Hadley, D. L. (1994). Effects of climate change on commercial building energy demand. *Energy Sources*, 16(3), 317–332. <https://doi.org/10.1080/00908319408909081>.
- Seoul Statistics. (2018). <https://data.seoul.go.kr/dataList/10582/S/2/datasetView.do>.
- Shen, Y., Tang, Y., & Dou, Q. (2018). The discovery of micro-blog users’ interest groups based on SSLOK-means clustering focus on big data improved by Calinski-Harabasz. In *Proceedings - 2nd international conference on data science and business analytics, ICDSBA 2018* (pp. 98–104). <https://doi.org/10.1109/ICDSBA.2018.00025>.
- Sriwanit, M., & Hokao, K. (2012). Effects of urban development and spatial characteristics on urban thermal environment in Chiang Mai metropolitan, Thailand. *Lowland Technology International*, 14(2), 9–22.
- Stewart, I. D., & Oke, T. R. (2012). Local climate zones for urban temperature studies. *Bulletin of the American Meteorological Society*, 93(12), 1879–1900. <https://doi.org/10.1175/BAMS-D-11-00019.1>.
- Stull, R. B. (2015). Chap 03: Heat. In *Meteorology for scientists and engineers, Brooks/Cole, Belmont CA, ISBN 978-0-534-37214-9, page 57 (Second edi, pp. 53–86)*. Brooks/Cole.
- Sung, H., Go, D., Choi, C. G., Cheon, S. H., & Park, S. (2015). Effects of street-level physical environment and zoning on walking activity in Seoul, Korea. *Land Use Policy*, 49, 152–160. <https://doi.org/10.1016/j.landusepol.2015.07.022>.
- Takebayashi, H., & Moriyama, M. (2009). Study on the urban heat island mitigation effect achieved by converting to grass-covered parking. *Solar Energy*, 83(8), 1211–1223. <https://doi.org/10.1016/j.solener.2009.01.019>.
- Tan, Z., Lau, K. K. L., & Ng, E. (2016). Urban tree design approaches for mitigating daytime urban heat island effects in a high-density urban environment. *Energy and Buildings*, 114, 265–274. <https://doi.org/10.1016/j.enbuild.2015.06.031>.
- Tran, H., Uchihama, D., Ochi, S., & Yasuoka, Y. (2006). Assessment with satellite data of the urban heat island effects in Asian mega cities. *International Journal of Applied Earth Observation and Geoinformation*, 8(1), 34–48. <https://doi.org/10.1016/j.jag.2005.05.003>.
- Voogt, J. A. (2002). In I. Douglas (Ed.), Vol. 3. *Urban Heat Island in, Encyclopedia of global environmental change*. John Wiley & Sons.
- Voogt, J. A., & Grimmond, C. S. B. (2010). Modeling surface sensible heat flux using surface radiative temperatures in a simple urban area. *Journal of Applied Meteorology*, 39(10), 1679–1699. <https://doi.org/10.1175/1520-0450-39.10.1679>.
- Woods, J., & Woods, J. (2012). Investigating the relationship between rooftop reflectance and zoning district in San Jose. *California Jordan Woods*, 5, 0–20.
- Wu, K., Ye, X., Qi, Z., & Zhang, H. (2013). Impacts of land use/land cover change and socioeconomic development on regional ecosystem services: The case of fast-growing Hangzhou metropolitan area, China. *Cities*, 31, 276–284. <https://doi.org/10.1016/j.cities.2012.08.003>.
- Yang, F., Lau, S. S. Y., & Qian, F. (2010). Summertime heat island intensities in three high-rise housing quarters in inner-city Shanghai China: Building layout, density and greenery. *Building and Environment*, 45(1), 115–134. <https://doi.org/10.1016/j.buildenv.2009.05.010>.
- Yeo, I. A., Yoon, S. H., & Yee, J. J. (2013). Development of an environment and energy Geographical Information System (E-GIS) construction model to support environmentally friendly urban planning. *Applied Energy*, 104, 723–739. <https://doi.org/10.1016/j.apenergy.2012.11.053>.
- Yu, S., Rhee, H.-J., Jung, C.-M., & Min, H.-K. (2017). Regulation of floor area ratio and its efficiency. *Journal of Korea Planning Association*, 52(6), 129–152.
- Zanon, B., & Verones, S. (2013). Climate change, urban energy and planning practices: Italian experiences of innovation in land management tools. *Land Use Policy*, 32, 343–355. <https://doi.org/10.1016/j.landusepol.2012.11.009>.
- Zhao, P., & Li, P. (2017). Reghinking the relationship between urban development, local health and global sustainability. *Current Opinion in Environmental Sustainability*, 25, 14–19. <https://doi.org/10.1016/j.cosust.2017.02.009>.
- Zhuang, Q., Wu, B., Yan, N., Zhu, W., & Xing, Q. (2016). A method for sensible heat flux model parameterization based on radiometric surface temperature and environmental factors without involving the parameter KB –1. *International Journal of Applied Earth Observation and Geoinformation*, 47, 50–59. <https://doi.org/10.1016/j.jag.2015.11.015>.
- Zitti, M., Ferrara, C., Perini, L., Carlucci, M., & Salvati, L. (2015). Long-term urban growth and land use efficiency in southern Europe: Implications for sustainable land management. *Sustainability (Switzerland)*, 7(3), 3359–3385. <https://doi.org/10.3390/su7033359>.